Received: 26 July 2022 | Revised: 25 September 2022 | Accepted: 30 September 2022

DOI: 10.1111/jnc.15699

Journal of Neurochemistry JNC The Official Journal of the International Society for Neurochemistry WILEY

ORIGINAL ARTICLE

Neurochemical, histological, and behavioral profiling of the acute, sub-acute, and chronic MPTP mouse model of Parkinson's disease

Matteo Santoro[1] | Paola Fadda[2] | Katie J. Klephan[3] | Claire Hull[1] | Peter Teismann[1] | Bettina Platt[1] | Gernot Riedel[1]

[1]Institute of Medical Sciences, University of Aberdeen, Aberdeen, UK

[2]Department of Neuroscience, University of Cagliari, Cagliari, Italy

[3]Newcastle University, School of Biomedical, Nutritional, and Sport Sciences, Newcastle upon Tyne, UK

Correspondence
Matteo Santoro, Stanford University, 1050 Arastradero road, Palo Alto, CA 94304, USA.
Email: santoro.matteo@outlook.com

Present address
Matteo Santoro, Department of Neurosurgery, School of Medicine, Stanford University, Palo Alto, California, USA

Katie J. Klephan, AccuRX, London, London, UK

Funding information
Tenovus Scotland

Abstract

Parkinson's disease (PD) is a heterogeneous multi-systemic disorder unique to humans characterized by motor and non-motor symptoms. Preclinical experimental models of PD present limitations and inconsistent neurochemical, histological, and behavioral readouts. The 1-methyl-4-phenyl-1,2,3,6-tetrahydropyridine (MPTP) mouse model of PD is the most common in vivo screening platform for novel drug therapies; nonetheless, behavioral endpoints yielded amongst laboratories are often discordant and inconclusive. In this study, we characterized neurochemically, histologically, and behaviorally three different MPTP mouse models of PD to identify translational traits reminiscent of PD symptomatology. MPTP was intraperitoneally (i.p.) administered in three different regimens: (i) acute—four injections of 20 mg/kg of MPTP every 2 h; (ii) sub-acute—one daily injection of 30 mg/kg of MPTP for 5 consecutive days; and (iii) chronic—one daily injection of 4 mg/kg of MPTP for 28 consecutive days. A series of behavioral tests were conducted to assess motor and non-motor behavioral changes including anxiety, endurance, gait, motor deficits, cognitive impairment, circadian rhythm and food consumption. Impairments in balance and gait were confirmed in the chronic and acute models, respectively, with the latter showing significant correlation with lesion size. The sub-acute model, by contrast, presented with generalized hyperactivity. Both, motor and non-motor changes were identified in the acute and sub-acute regime where habituation to a novel environment was significantly reduced. Moreover, we report increased water and food intake across all three models. Overall, the acute model displayed the most severe lesion size, while across the three models striatal dopamine content (DA) did not correlate with the behavioral performance. The present study demonstrates that detection of behavioral changes following MPTP exposure is challenging and does not correlate with the dopaminergic lesion extent.

Abbreviations: DA, Dopamine; DAT, dopamine transporter; ENS, enteric nervous system; HPLC, high performance liquid chromatography; LDB, light-dark box; L-DOPA, l-3,4-dihydroxyphenylalanine; MAO_B, monoamine oxidase B; MPP^+, 1-methyl-4-phenylpiridinium; MPTP, 1-methyl-4-phenyl-1,2,3,6-tetrahydropyridine; MS, motor symptoms; NMS, non-motor symptoms; PD, Parkinson Disease; RRID, Research Resource Identifier (see scicrunch.org); SNpc, Substantia Nigra pars compacta; STR, Striatum.

KEYWORDS
1-methyl-4-phenyl-1,2,3,6-tetrahydropyridine, behavioral symptoms, dopamine, dopaminergic neurons, nigrostriatal lesion

1 | INTRODUCTION

Parkinson's disease (PD) manifests itself in an age-dependent manner due to spreading of Lewy bodies in the brain and progressive neurodegeneration. Modelling PD in rodents and primates has proven challenging despite the numerous pharmacological and genetic tools available. The general consensus about the ideal animal model of PD is that it should present the following characteristics: (1) a fully formed dopaminergic system at birth; (2) a gradual loss of neurons during adulthood that significantly affects the *substantia nigra pars compacta* (SNpc) region and other nuclei and traits; (3) motor symptoms (MS) arising from the loss of dopamine (DA) in the *striatum* (STR); and (4) pathological proteinaceous inclusions that are positive to α-synuclein (α-syn). To date, there is no animal model that can fully recapitulate all the pathological hallmarks of PD. Currently, the model that most closely mimics PD is the pharmacological administration of 1-methyl-4-phenyl-1,2,3,6-tetrahydropyridine (MPTP) to non-human primates (Cohen et al., 1984; Forno et al., 1986). A quick PubMed research for publications containing the acronym MPTP in the title showed that between 1997 and 2016 the number of publications on PubMed rose steadily from about 62 to 161 per year. Nonetheless, in mice the administration of MPTP produced many inconsistencies in terms of histology, neurochemistry and behavior depending on strain, age and sex (Antzoulatos et al., 2010; Pothakos et al., 2009; Quinn et al., 2007; Sedelis et al., 2000; Sedelis et al., 2001; Tillerson et al., 2002). Today's lack of behavioral guidelines on the MPTP mouse model of PD is due to the large number of discordant publications on one hand, and the nature of behavioral readouts characterized by high variability and poor reproducibility on the other (Luchtman et al., 2009; Pothakos et al., 2009; Rozas et al., 1998). Such inconsistencies prompted us to quantify the extent of the MPTP lesion at the nigrostriatal level and determine whether the behavioral performance is affected by the MPTP toxicity. Adding to this, the emergence of multiple MPTP administration regimens, administration routes, and the use of adjuvants (Irwin et al., 1987; Lau et al., 1990; Zuddas et al., 1989) make the picture even more convoluted. Caution must also be taken when assessing certain transitory behavioral traits occurring prior to the stabilization of the MPTP neurotoxic lesion. Such changes give rise to behavioral patterns not necessarily related to DA loss but instead might be the result of acute MPTP toxicity as well as transient compensatory mechanisms taking place in the basal ganglia (Huang et al., 2017). We have found four reports in total comparing behavioral anomalies among various MPTP regimens (Gibrat et al., 2009; Goldberg et al., 2011; Luchtman et al., 2009; Petroske et al., 2001). In 2001 Petroske and colleagues compared the sub-acute (five intraperitoneal (i.p.) injections of 30 mg/kg MPTP/day) versus a chronic regimen (10 i.p. doses of 25 mg/kg every 3.5 days) combined with 250 mg/kg of the adjuvant probenecid supposed to reduce renal excretion of MPTP. They reported fluctuating changes in DA content in the STR for the sub-acute regimen but opted for the chronic model claiming that variability is smaller in favor of a greater lesion extent, which led to the appearance of motor deficits using the Rotarod apparatus (Petroske et al., 2001). Lutchman and colleagues have carried out a more extensive behavioral characterization using the same MPTP regimens in addition to a third acute MPTP model (four i.p. doses of 20 mg/kg 2 h a part). Despite remarkable differences noted across the three regimens in relation to the behavioral performance, they failed to identify PD relevant behavioral endpoints robust enough to discriminate between healthy controls and MPTP treated subjects. The only exception was the presence of an impaired RotaRod performance in the acute and chronic/probenecid models. Noteworthy, behavioral testing was carried out only 2 days after the last MPTP injection, allowing no time for the establishment of a dopaminergic lesion and the dissipation of the acute toxic effects of the MPTP (Luchtman et al., 2009). A more ambitious study designed to investigate the cumulative effects of MPTP in C57BL/6J mice used a progressive MPTP regimen (28 incremental i.p. MPTP injections ranging from 4 mg/kg to 32 mg/kg per day). Once again, most of the behavioral testing was carried out during or only 2 days after the last MPTP injection which resulted in failure to identify any reliable behavioral deficits in olfaction, rearing, and parallel rods. The only exception was the reduced number of rearings reported after a 3-week wash-out period (Goldberg et al., 2011). In synthesis, the reports generated on MPTP are based on a large and variable number of MPTP dosages, experimental conditions, mouse strains, and behavioral assessments making it extremely difficult to pinpoint the underlying neuropathological mechanism responsible for the manifestation of certain behavioral deficits.

Today, PD is seen as a heterogeneous multi-systemic disorder with clinically distinct MS and non-motor symptoms (NMS) (Klingelhoefer & Reichmann, 2017) with the appearance of MS (Tremor, Rigidity, Akinesia and Postural instability/TRAP) allowing the clinical diagnosis of PD (Jankovic, 2003; Rodriguez-Oroz et al., 2009). So far, several attempts to replicate the resting tremor in PD mouse models have failed with the exception of motor and gait alterations being well documented in the sub-acute MPTP regime (Wang et al., 2012). Symptoms such as akinesia, dyskinesia, and bradykinesia entail inability to initiate voluntary movements, presence of uncontrollable involuntary movements, and slowness of movements, respectively. With this regard, a test that accounts for neuromuscular strength, coordination, and rigidity is the inverted grid/traction test for which we have previously developed an innovative analysis algorithm for the identification of movement patterns. Yet, even this highly sensitive tool did only reveal a small impairment in coordination following acute MPTP intoxication (Niewiadomski et al., 2016b).

The incidence of NMS in PD patients ranges from 88% (Shulman et al., 2001) up to 98.6% (Barone et al., 2009). To date, the neuropathological bases of NMS are not fully understood, and in addition to the reduced DA content, altered levels of serotonin (5-HT), norepinephrine and acetylcholine are likely to be the

underlying cause (Bohnen et al., 2015; Grimbergen et al., 2009; Lou et al., 2015; Olivola et al., 2014). Varying between epidemiological studies, occurrence of depression ranges from 35% to 58% and anxiety, panic attacks, and other phobias appear in 40% of PD cases (Pontone et al., 2011; Richard, 2005). Attempts to detect depression and psychosis in MPTP mouse models have met with little success (Okano et al., 2019, Li et al., 2018). Among the NMS, dementia is one of the most disabling; with up to 80% of PD patients being affected during advanced stages of the disease (Aarsland et al., 2003), while mild cognitive impairment occurs in 25% of non-demented PD patients at any time (Aarsland et al., 2010). Cognitive impairments in the MPTP mouse model have been reported using the water maze in a chronic MPTP/probenecid model (Carta et al., 2013) but not after the sub-acute injection regime (Wang et al., 2021). Passive avoidance tests highlighted memory deficits only in the sub-acute model so far (Haga et al., 2019; Zhao et al., 2017). Disorganized sleep and alterations in circadian and ultradian rhythms are very common in PD with prevalence ranging from 70 to 90% (Claassen et al., 2010; Svensson et al., 2012). Nonetheless, such alterations have not been found in the acute and chronic mouse models of MPTP (Fifel et al., 2013; Tanaka et al., 2012). For a more comprehensive review of the behavioral tests and paradigms reported on the MPTP mouse models see Kasahara et al. (2017) and Sedelis et al. (2001).

Here, we revisited the issue of multiple MPTP injection regimes and their effects on (a) behavioral testing and (b) biochemical and histological quantification of the lesion extent, followed by (c) a correlation analyses between selected proxies. Behavioral testing was only carried out after full-blown establishment of the dopaminergic lesions based on existing literature. From highest to lowest the lesion extent appeared in the following order acute>chronic>sub-acute model combined with impairments in gait and non-associative habituation to a novel environment. Some issues with balance were identified for the chronic model while the sub-acute regimen induced generalized hyperactivity. A novel finding for all models was the significant increase in food and water intake posing questions regarding the metabolic impairment and/or alteration of the gastrointestinal apparatus.

2 | METHODS

2.1 | Animals

Male C57BL/6 mice 8 weeks old were purchased from Charles River laboratories (RRID:IMSR_CRL:027). Mice between 8 and 10 weeks of age present highest expression levels of the monoamine oxidase B (MAO_B) enzyme responsible for the reduction of MPTP to its toxic metabolite 1-methyl-4-phenylpiridinium (MPP^+) (Jackson-Lewis & Przedborski, 2007). Unless otherwise specified, animals were group-housed (four/five per cage) in environmentally controlled rooms (19.5–21.5°C, 60–65% relative humidity) with a 12-h light/dark cycle (lights on at 7 a.m.) and transition phases of 60 minutes (min) simulating dawn and dusk. Mice were held in open housing Macrolon type II cages (Techniplast, cat. n.: 1284 L) with corncob bedding and free access to water and food (CRM, Special Diets service, cat. n.: 801151). Wood chippings, paper wool, and cardboard tubes were used as environment enrichment (1 cage change per week, handling by tail lift). All the procedures including animal housing and holding were performed in agreement with the United Kingdom Animal (Scientific Procedures) Act 1986, the EU directive 63/2010EC, the Federation of European Laboratory Animal Science Association (FELASA) guidelines (Guillen, 2012) and further approved by the local Ethics Review Committee.

2.2 | MPTP regimens and cohorts

MPTP hydrochloride (MPTP·HCl) was purchased from Sigma Aldrich (Sigma, cat. n.: M0896). MPTP handling, and injections were carried out following the guidelines and safety procedure described by Jackson-Lewis and Przedborski (Jackson-Lewis & Przedborski, 2007). Three different MPTP regimens were administered:

1. *Acute* - i.p. injection of 20 mg/kg of MPTP (free base) or 0.9% saline solution every 2 h for a total of four injections in 1 day. MPTP $n = 10$, saline $n = 12$, Figure 1a (Przedborski & Vila, 2003). The attrition rate in the MPTP treated group was of 44% with a reduction of sample size from 18 to 10.
2. *Sub-acute* - i.p. injection of 30 mg/kg of MPTP (free base) or 0.9% saline once a day for five consecutive days. MPTP $n = 17$, saline $n = 12$, Figure 1b (Burns et al., 1983; Przedborski & Vila, 2003). The attrition rate in the MPTP treated group was of 5% with a reduction of sample size from 18 to 17.
3. *Chronic* - i.p. injection of 4 mg/kg MPTP (free base) or 0.9% saline once a day for 28 consecutive days. MPTP $n = 11$, saline $n = 9$, Figure 1c (Bezard et al., 1997b; Huang et al., 2017). The attrition rate in the MPTP treated group was of 5% with a reduction of sample size from 12 to 11.

Trained personnel performed the i.p. injections into the upper peritoneum to avoid bowel puncture. Cages were equipped with a heating pad that prevented loss of body heat following the MPTP injections. None of the deceased mice due to the MPTP systemic toxic effects have been replaced. In addition, mushed food and hydrogel were temporary placed on the floor of the cages for 48 h following the last MPTP injections. No randomization was performed to allocate subjects in the study. Mice were arbitrarily allocated to the six groups.

2.3 | Behavioral testing

The behavioral characterization of the three MPTP models (acute, sub-acute, and chronic; see Figure 1d) began 2 days after establishment of full-blown lesion at nigrostriatal level. The time window necessary for the establishment of the lesion extent is equal

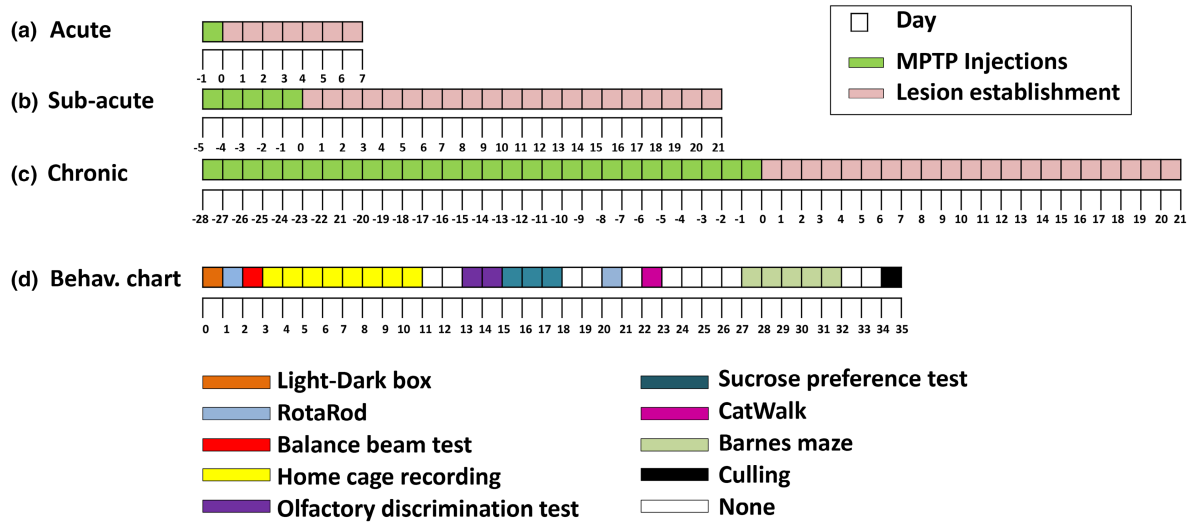

FIGURE 1 Flow charts of the three MPTP regimens and behavioral tests. (a) Acute regimen: nigrostriatal lesions establish during 7 days post MPTP. (b) Sub-acute and (c) chronic MPTP administration regimens with 21 days for emergence of the full-lesion extent. (d) Series and sequence of behavioral tests applied with minimal invasive/aversive paradigms administered first.

to 7 days for the acute regime and 21 days for the sub-acute and chronic regimen following the last MPTP injection (see Figure 1a–c) (Bezard et al., 1997b; Burns et al., 1983; Przedborski & Vila, 2003). All behavioral experiments were performed on weekdays from 9 a.m. to 4 p.m. except for the PhenoTyper measurements consisting of seven consecutive days of uninterrupted home cage video recording. Behavioral apparatuses were cleaned with 70% ethanol between animal trials. All the behavioral testing and analyses were done with the operator being blind to the study treatments.

2.4 | Tests for stamina, balance, and gait

2.4.1 | Rotarod

We tested the stamina of the animals using an accelerating Rotarod (Model 47 700, Rat Rotarod) consisting of a furrowed drum with a 6 centimeters (cm) diameter and four lanes each 8.6 cm wide. Subjects were tested at 4 and 21 days after the establishment of the lesion. Mice were placed on the Rotarod at an initial speed of two rotations per minute (rpm) accelerating to the maximum speed within the first 30 seconds (sec) (8 rpm—first trial; 12 rpm—second trial). The trial was terminated when the animals either fell off the drum or when the cut-off time point of 600 sec was reached. Animals that fell off within the initial 30 s were reassessed a second time only. Latency to fall was recorded and considered as a proxy of physical endurance (Hull et al., 2020).

2.4.2 | Balance beam test

The balance beam test is used to assess motor coordination and balance in rodents. In our study, mice were required to traverse three 50 cm long circular beams with different cross-sectional diameter in the following order: 28, 11, and 5 millimeters (mm). Beams were placed at 30 cm from the ground and inclined at 30°. Beams were covered with surgical tape to offer sufficient grip and soft bedding was placed underneath the beams. Latency to traverse the beam and number of foot slips were recorded manually during one trial only. The test was ended either when the animal had completed the task or when the cut-off point of 30 sec was reached without completion of the task.

2.4.3 | CatWalk

Gait assessment was performed using the CatWalk XT apparatus and the software CatWalk XT 10.0 (Noldus IT, Wageningen, The Netherlands). The operation principles of the CatWalk were described elsewhere (Wang et al., 2012). During the trial mice were allowed to walk freely across the glass platform (dimension: length 40 cm, width 10 cm) in an unforced manner for three times. Runs across the walkway were considered successful only when the run duration was between 0.5 and 5 s. Only one run per trial was analyzed based on duration and continuity of the run. Table 1 lists the definitions of the different gait parameters used in this study based on previous literature (Wang et al., 2012).

2.5 | Anxiety and anhedonia

2.5.1 | Light–dark box (LDB)

The LDB apparatus consists of two Perspex® boxes: a bigger open white compartment lid (30 × 30 × 30 cm, 208 lux) and a smaller dark compartment (30 × 20 × 25 cm, 0.1 lux) (George et al., 2008). The

TABLE 1 Definition of parameters considered during the quantitative analysis of gait acquired with the CatWalk/CatWalk XT system

Gait parameter	Definition
Average speed (cm/sec.)	Speed of the animal
Cadence (step/sec.)	Number of steps per second
Base of support (cm)	Distance between either front or hind paws
Swing speed (cm/sec.)	Speed of the paw during swing
Stride length (cm)	Distance between two consecutive placements of the same paw
Stance (sec.)	Contact duration of the paw with the glass platform
Step cycle (sec.)	Time between two consecutive contacts of the same paw
Duty cycle (%)	Stance reported as percentage of step cycle
Regularity index (%)	Number of normal step sequence patterns relative to total number of paw placements

two compartments were connected by a hemi-circular aperture at floor level with a diameter of 7.5 cm. Animals were placed in the light compartment and allowed to freely explore the apparatus for 10 min. Latency to first entry into the dark compartment and time spent in the light compartment were video recorded using the software Ethovision XT 6 (Noldus IT).

2.5.2 | Olfactory discrimination test

Rodents tend to spend more time on sawdust impregnated by their own body scent in comparison to fresh sawdust (Prediger et al., 2006). The apparatus used in the present test consisted of one Perspex® box divided into two compartments (43 cm length × 26 cm wide) by a Perspex® wall with a communicating aperture at floor level (10 × 10 cm) allowing the mouse to freely move between the two. One compartment contained fresh sawdust (non-familiar compartment), whereas the other compartment was filled with sawdust from the home cage of the tested mouse (familiar compartment). Mice were individually housed for ≥36 h prior to the test (Prediger et al., 2006). Animals were placed in the middle of the non-familiar compartment and allowed to freely explore the apparatus for 15 min. Time spent in each compartment, latency to first entry into familiar compartment and distance moved were measured using a video camera and recorded by Ethovision XT 6 software (Noldus IT).

2.5.3 | Sucrose preference test

The test is based on the natural preference of rodents for sweet liquid solutions over water. The preference for the sucrose solution is related to the ability to feel pleasure and consequently to hedonic behavior. Animals were individually housed in wire-top shoe-box cages and tested over a period of 48 h. During the test two bottles were presented to the animals on top of the wire lid, one containing water, the other containing sucrose solution at 1% (sucrose Fisher scientific cat. n.: AAJ65148A1). Animals had free access to the two bottles and food. The bottles were swapped after a period of 24 h to avoid side preference bias. Water and sucrose consumption were recorded manually at two different time points (24 and 48 h). Preference for the sucrose solution (SP) expressed as a percentage was determined by dividing the volume of sucrose consumed by the total volume of liquid drunk as per Equation 1 (Strekalova et al., 2006).

$$SP = \frac{Volume\ of\ sucrose}{Total\ liquid\ intake} \times 100 \quad (1)$$

2.6 | Home cage recording and habituation to novel environment

Mice were individually housed in PhenoTyper home cages supported by the multi-arena software Ethovision 3.1Pro (Noldus IT) as described previously (Bains et al., 2017; Robinson et al., 2013). Each PhenoTyper cage was 30 × 30 cm with an infrared-sensitive camera and an infrared light source positioned at the top of each cage. Behavioral activity was tracked for 7 consecutive days with a sampling rate of 12.5 Hz. To measure habituation, we used locomotion as an indicator of the animal's response to the new environment measured during the first 3 h since housing in the PhenoTyper cages. Data were extracted in time bins of 10 min and tested against the one-phase exponential decay algorithm $Y = (Y_0 - Plateau) \bullet e^{(-K \bullet t)} + Plateau$, where Y = distance covered at any given time t, K = decay constant, and Y_0 = motor activity at time $t = 0$. The locomotor activity of individually housed mice strongly correlates with the dark/light phases; therefore, in the present study locomotion was also used as a parameter to assess circadian rhythms over a period of 114 h, from day 3 to day 7. During the habituation phase activity data were reported as distance in cm per 10-min time bins over a period of 3 h, while circadian rhythm data were reported in cm per 2-hour time bins for 5 consecutive days. Consumption of food and water was measured manually by weighing the food hoppers at day 1 and daily from day 4 to day 7.

2.7 | Cognition

2.7.1 | Barnes maze

Cognitive differences between MPTP and saline injected animals were sought using the Barnes maze apparatus (O'leary & Brown, 2012). The apparatus consists of a circular arena of grey color made of stainless steel (Ugo Basile, Gemonio, Italy) with a diameter of 120 cm elevated 80 cm above the floor and containing sixteen holes (with a diameter of 8 cm) equidistantly distributed along the perimeter of the arena 2.5 cm away from the edge. The platform was brightly illuminated using four

floodlights of 500 volts each to provide an aversive stimulus that will motivate the mice to locate the escape box. The escape box made of black Perspex was placed under the same hole (North hole) throughout the trials. Various visual clues were placed in the environment surrounding the maze. Animals were released into the center of the arena and tested over a period of 5 days; on day 1 animals were habituated to the maze through free exploration of the apparatus for 5 min. During habituation (day 1), curtains were drawn around the maze and if animals failed to locate the escape box (within 120 s), they were gently guided towards it. During the acquisition phase (from day 2 to day 5) the curtains were removed, and animals were tested twice daily with an inter trial interval of 15–20 min, for four consecutive days. Released into the center of the arena, mice who failed to locate the escape box within 120 s were guided to the escape box by the experimenter. During the training phase, primary path length and speed were used as primary endpoints to measure the visuospatial learning ability of the mice. Software ANY-MAZE (Stoelting) was used for video-recording, data acquisition, and data extraction.

2.8 | Assessment of MPTP-induced lesion extent

2.8.1 | Tissue harvesting

For lesion quantification all animals in each group were sacrificed after completion of the behavioral battery (Figure 1). Animals were quickly decapitated, brains removed, *striata* isolated from one hemisphere and immediately snap frozen in liquid nitrogen for high-performance liquid chromatography (HPLC) analysis. The rest of the brains were post fixed for 24 h in 4% paraformaldehyde and cryopreserved in 0.1 M phosphate buffer (PB) containing 30% sucrose for histology assessment. Given that DA levels in the STR can fluctuate quite dramatically following environmental changes and stressors (Shimada, 1981; Shum et al., 1982), it is important to adopt handling and culling methods that minimize stress, i.e. decapitation or cervical dislocation (Shum et al., 1982; Zaczek & Coyle, 1982). The operators were maintained blind to the study treatment during the assessment of lesion extent.

2.8.2 | Stereological cell counting of nigral tyrosine hydroxylase (TH)-positive neurons

An average of 50 coronal brain sections 30 μm thick were obtained from ventral midbrain covering a brain portion of about 1.44 mm ranging between −3.88 and −2.46 from Bregma according to the Paxinos and Franklin's brain atlas (Paxinos & Franklin, 2019) using a Leica CM1850 cryostat (Leica Microsystems). Every fourth coronal section was selected for a total of 12 sections per brain. The free-floating staining procedure was carried out in 0.1 M phosphate buffer (PB). Following inhibition of endogenous peroxidases (10% Methanol and 3% hydrogen peroxide), unspecific binding sites were blocked with 5% normal goat serum (NGS, Vector Laboratories, UK, RRID:AB_2336615). Sections were then incubated with rabbit polyclonal anti-TH (1:1000 Millipore, UK, RRID:AB_390204) in 2% NGS, for 48 h at 4°C. After washing, sections were incubated with biotinylated goat polyclonal anti rabbit secondary antibody (1:200, Vector Laboratories, RRID:AB_2313606) in 2% NGS, for 1 h at 21°C. Sections were then incubated with Vectastain ABC standard kit™ (Vector Laboratories, RRID:AB_2336818), as per manufacturer instructions. Revelation of TH positive cells was done using a solution containing 0.30 g of Trizma pre-set crystal™, (Millipore Sigma, UK, cat. n.: T0569) 12.5 mg of 3,3′-diaminobenzidine (DAB method, Sigma, UK, cat. n.: D8001), 10 mg of NH_4Cl, 225 mg of Glucose oxidase (Sigma) and 50 mg of D-(+)-glucose (Sigma) in 25 ml of water. Sections were then counterstained with Lauth's violet (Nissl stain, thionin acetate, Sigma, Cat. n.: 88930), dehydrated and coverslipped with Entellan medium (VWR Chemicals, Cat. n.: 1.07961.0100). TH- and Nissl-positive neurons in the SNpc were stereologically counted in bright field via optical fractionation method using the Zeiss Axio Imager M1 microscope (Carl Zeiss) and the software Stereo Investigator Version 7 (MBF Bioscience). Endpoints are presented as total number of cells extrapolated based on the sample size. Size of the sampling grid covered 20% of the SNpc and area of each section and the thickness is defined, respectively, by Equations 2 and 3 (A = area, t^-_{Q-} = average section thickness, t_i = section thickness at site I, Q_i = particles counted, m = number of sections).

$$A = \frac{1}{2}(x_0y_n - x_ny_0) + \sum_{i=1}^{n-1}(x_{i+1}y_i - x_iy_{i+1}) \quad (2)$$

$$t^-_{Q-} = \frac{\sum_{i=1}^{m} t_iQ_i^-}{\sum_{i=1}^{m} Q_i^-} \quad (3)$$

2.8.3 | Quantification of striatal TH-positive fibers

Every eighth section (30 μm thick) was collected for an average of thirteen striatal sections per brain (−1.70 to +1.54 from Bregma). Striatal TH-positive fibers were stained as per TH-positive cells in SNpc using the Vectastain ABC Elite kit™ (Vector Laboratories, RRID:AB_2336826). Sections were then dehydrated and mounted on slides using Entellan medium (VWR Chemicals, Cat. n.: 1.07961.0100). Optical density assessment of TH-immunoreactive striatal fibers was conducted on scanned images (Hewlett Packard Scanjet G3110, Bracknell) using Scion image software and the Equation 4 where "y" is the optical density, "x" is the grey value and "255" is the value attributed to the maximum intensity i.e. black (Version 4.0.3.2 Scion Corporation). Background values yielded by cortical regions were subtracted to the striatal values. Raw optical density values from each section were averaged per each brain.

$$y = log10\left(\frac{255}{255 - x}\right) \quad (4)$$

2.8.4 | HPLC analysis of neurochemicals

Striatal content of DA, serotonin (5-HT) and their metabolites 3,4-dihydroxyphenylacetic acid (DOPAC), homovanillic acid (HVA),

and 5- hydroxyindoleacetic acid (5-HIAA) was quantified using the Thermo Fisher HPLC system consisting of a solvent rack SRD3400, isocratic pump ISO-3100A, autosampler WPS-3000 TSL analytical and computer interface UCI-50 (Dionex). The method was previously described (Nuber et al., 2011). *Striata* were sonicated in 1.5-ml tubes using the Bandelin Sonoplus GM2070 sonicator (Germany) in 0.1 M perchloric acid aqueous solution (1:20 wt/vol). Samples were then centrifuged at 20 784 *g* (Mikro 200R Hettich). The mobile phase used contained: 50 mM of sodium acetate, 35 mM of citric acid, 105 mg/L of sodium octane sulfonic acid (Fisher Scientific), 48 mg/L of ethylenediaminetetraacetic acid (EDTA, VWR chemicals), and 10% methanol (Fisher Scientific). An isocratic flow of 0.2 ml/min and the analytical column Acclaim PA2, 3 μm, 2.1 × 150 mm (Dionex, Acclaim, Cat. n.: 063189) were used to separate the neurotransmitters that were then detected with an electrochemical analytical cell ESA 5011A set at 650 mV connected to the ESA Coulochem II detector (guard cell ESA 5020). Data regarding the striatal content of DA, 5-HT and their metabolites were gathered using the Chromeleon chromatography management system (Thermo Fisher, UK) and reported as both nanograms (ng) or picograms (ρg) per milligrams (mg) of brain tissue.

2.9 | Statistical analysis

Group size was empirically determined based on previous observations carried out in our laboratory, which have proven to be statistically robust with regard to the quantification of lesion size at nigrostriatal level (Santoro et al., 2016). Statistical power of the study was determined *a posteriori* using Equation 5 with α set at 0.05 and β set at 0.2.

$$Power = \Phi\left\{ -Z_{1-\alpha/2} + \frac{\Delta}{\sqrt{\sigma_1^2/n_1 + \sigma_2^2/n_2}} \right\} \quad (5)$$

Equation 5 was developed based on previously published work (Levine & Ensom, 2001; Rosner, 2011) where n_1 = samples size of the control saline group, n_2 is the samples size of the MPTP group, Δ = is the absolute difference between the two means, σ_1 and σ_2 variance of saline and MPTP mean, respectively, α probability of type I error, Z critical Z value for a given α, and Φ function converting the critical Z value to power. Power is reported in supplementary material (Table S1) for pairwise comparison of the following nigrostriatal lesion endpoints: striatal DA content, striatal dopamine fibers (TH immunoreactive) and SNpc TH-positive cells. Post-hoc power is mathematically expressed as the probability of type II error (β) and reported as percentage of 1-β. All the primary nigrostriatal lesion data sets had a statistical power between 95.2 and 100% (Table S1). Prior to the implementation of any statistical comparison or correlation, the D'Agostino and Pearson omnibus test was applied to confirm normal distribution of all data sets; while Grubbs' test was used to detect significant mathematical deviations of single data points from the mean (outliers) (Grubbs, 1969; Stefansky, 1972). The true sample size per each group has been reported in each bar graph, line graph, or scatter plot after the removal of the outlier based on Grubbs' test only (α = 0.05). Any data point loss due to experimental reason is clearly stated in the figure caption along with the experimental group size prior to any outlier exclusion. No animals were excluded based on behavioral performance unless mice were not able to complete the task. Such occurrences are clearly reported in the figure captions. Due to the different number of injections, duration, and timelines required for the stabilization of the MPTP neurotoxic lesion, each MPTP regimen constitutes an independent experiment. Hence, to evaluate significant changes induced by MPTP treatment in each cohort, the two-tailed student's *t*-tests was used, except for pairwise comparison of the lesion extent at nigrostriatal level where the one-tailed student's *t*-test was used to assess the scale of reduction of TH-positive fibers, cells, and striatal catecholamines. Comparisons to chance level was performed using the one-sample *t*-test for sucrose preference, LDB, and olfactory discrimination test, with the hypothetical chance level set at 50%. Correlation analyses using Pearson's test was conducted on all data sets to determine any relationship between lesion extent and behavioral performance. To compare the MPTP effects across the three regimens, data sets were normalized to their control groups and then compared using the parametric factorial analysis of variance including the saline control groups (one-way ANOVA). This approach accounts for inter-experiment variability by normalizing the data sets against the saline control groups allowing to seek a size effects induced by each MPTP regimen. More importantly, Bonferroni *post-hoc* analyses were applied to MPTP cohorts only to reveal significant differences across the treated cohorts. If data sets were characterized by two independent variables, two-way ANOVA was used followed by applicable *post-hoc* tests as described above. Alpha was always set at 5%. Statistical analyses were performed using Prism version 5.1 (GraphPad).

3 | RESULTS

3.1 | Quantification of the nigrostriatal lesion across the three MPTP models

The neurotoxic cell death induced by MPTP occurs in a rostro-caudal fashion spreading from striatal nerve terminals to the cell bodies located into the SNpc (Chen et al., 2008). The data presented in Figure 2 show the neurotoxic effects of MPTP on the following: (1) content of DA and its metabolites in the STR, (2) density of TH-positive fibers in the STR, and (3) number of TH and Nissl-positive neurons in the SNpc. The data were normalized to each saline counterpart, while the three saline groups have been condensed into a single bar with three different standard deviation (SD) bars, one per each saline group. The HPLC neurochemical quantification of DA content in the STR (see Table S2 for raw data and Table S3 for variability) revealed significantly lower levels across the three MPTP regimes (Figure 2a). The acute MPTP regimen induced the greatest reduction in DA content by approximately 68% (t = 4.53, df = 20, p = 0.0001, one-tailed *t*-test), compared with the chronic regime

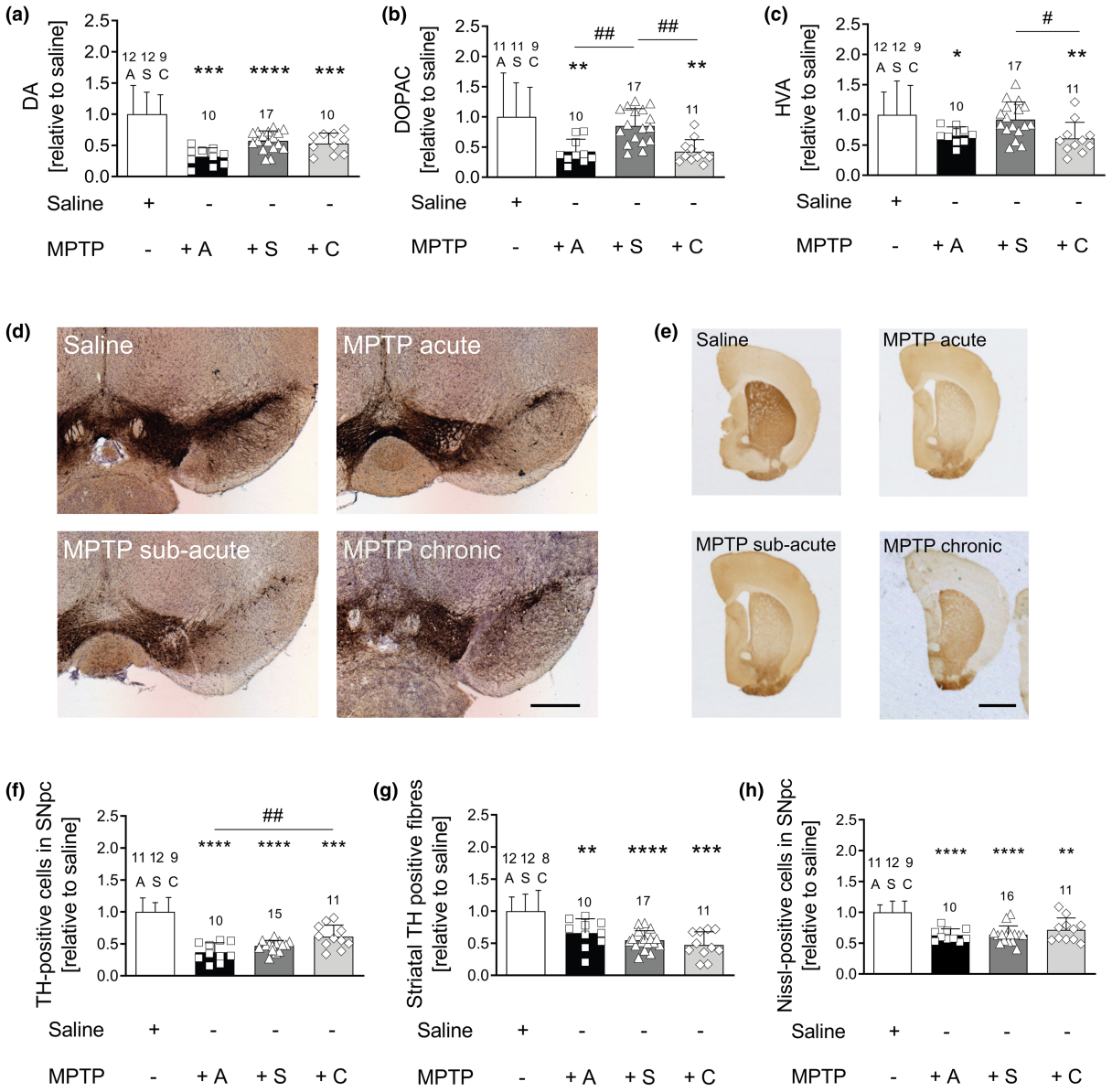

FIGURE 2 Lesion extent quantification across the three MPTP models. Post-mortem histopathological and neurochemical assessment of the MPTP neurotoxic lesion at nigrostriatal level. Quantitative data are normalized to the respective saline control groups for direct comparison. Data are expressed as mean, SD (a) dopamine (DA), (b) 3,4-dihydroxyphenylacetic acid (DOPAC) and (c) homovanillic acid (HVA) levels measured in the *striatum* by HPLC. (d) 3,3′-diaminobenzidine (DAB) immunostained coronal brain sections for tyrosine hydroxylase (TH)-positive neurons in the *substantia nigra pars compacta* (SNpc) (scale bar = 0.5 mm) and (e) TH-positive fibers at striatal level (scale bar = 1 mm). (f) Number of stereologically counted TH-positive neurons in the SNpc and (g) Striatal TH-positive fibers quantified via optical density analysis. (h) Number of Nissl-positive neurons in the SNpc. Comparison between relative saline control groups and each MPTP regimen cohort was performed using two-tailed student t-test with confidence of interval at 95% $^{*}p<0.05$, $^{**}p<0.01$, $^{***}p<0.001$, $^{****}p<0.0001$. All the cohorts pertaining to the MPTP models were compared using one-way ANOVA followed by Bonferroni post-hoc tests where applicable to seek for differences among MPTP cohorts only $\#p<0.05$, $\#\#p<0.01$. A = acute, saline $n = 12$, MPTP $n = 10$; S = Sub-acute, saline $n = 12$, MPTP $n = 17$; C = chronic, saline $n = 9$, MPTP $n = 11$. n = number of mice. For the Nissl−+and TH−+−cells data set the acute saline group and the sub-acute MPTP group have one missing datapoint due to low quality of the tissue. For striatal TH−+ fibers the chronic saline group has one missing data point due to low quality of the tissue. Actual sample size after outliers exclusion is stated on top of each bar chart.

(43% $t = 4.24$, df = 17, $p = 0.0003$) and the sub-acute dosage of MPTP (43.7% $t = 4.3$, df = 27, $p<0.0001$). DA levels were equally lowered by the MPTP treatment across all three regimens (one-way ANOVA: $F_{[5,64]} = 11.81$, $p<0.0001$); with the *post-hoc* analysis revealing no differences among the three MPTP treated groups.

The metabolite DOPAC (Figure 2b) was significantly reduced in both the acute and chronic model, but not in the sub-acute regimen ($t = 1.202$, df = 26, $p = 0.24$) suggesting perhaps an increased turnover of DA as compensatory mechanism, which was also reported elsewhere (Heikkila et al., 1984). Striatal DOPAC was lowered by

57% and 58% following the acute ($t = 3.25$, df = 19, $p = 0.0042$) and chronic regimen, respectively, ($t = 3.59$, df = 18, $p = 0.0021$) with the one-way ANOVA revealing a significant difference ($F_{[5,63]} = 6.66$, $p < 0.0001$) (Figure 2b). Likewise, the levels of the downstream metabolite HVA (Figure 2c) were significantly reduced after the acute and chronic MPTP treatment (acute: $t = 2.66$, df = 20, $p = 0.015$; chronic: $t = 3.28$, df = 18, $p = 0.0042$) with a significant MPTP effect ($F_{[5,65]} = 4.10$, $p < 0.0027$). The ratios of DOPAC/DA and HVA/DA shown in the Table S2 are indicators of DA catabolism and therefore DA turnover. A significant increase in DA turnover was observed in the sub-acute model as per increased ratios of DOPAC/DA ($t = 4.62$, df = 26, $p < 0.0001$) and HVA/DA ($t = 9.66$, df = 26, $p < 0.0001$). By contrast, weaker effects were observed in the acute and chronic treatment with significant changes observed only for HVA/DA and DOPAC/DA ratios, respectively (Table S2). Striatal levels of 5-HT and 5-HIAA remained unchanged as well as the turnover of the serotonin across the three different models (Table S2). The reduction of DA is undoubtedly the consequence of the MPTP toxicity upon dopaminergic fibers and TH-positive cells in striatal and nigral regions, respectively (Figure 2d–h). A significant reduction in TH-positive cells was observed consistently for all treatments (acute: >60%, $t = 7.7$, df = 19, $p < 0.0001$; sub-acute: >50%, $t = 12.29$, df = 25, $p < 0.0001$ and chronic: >40%, $t = 4.25$, df = 18, $p = 0.0002$ - Figure 2d–f) with the greatest lowering evoked by the acute MPTP administration. One-way ANOVA revealed an overall significant main effect of treatment ($F_{[5,62]} = 34.62$, $p < 0.0001$) with the *post-hoc* analysis yielding a significant difference between the acute and chronic model ($t = 3.33$, $p < 0.01$). Likewise, all MPTP regimes reduced TH-fibers (Figure 2e–g). Compared with chronic and sub-acute administration, a severe loss of TH-positive cells in the acute treatment was not mirrored by the reduction in TH-positive fibers. In fact, in the acute model the loss of TH-positive cells was only ≈35% ($t = 3.551$, df = 20, $p = 0.001$ compared with saline) and was the lowest of all the MPTP models. Likewise, the severe lowering of TH-fibers in the chronic model (>50%, $t = 4.345$, df = 17, $p = 0.0002$) was accompanied by a weaker reduction in TH-positive somata (≈38%, $t = 4.248$, df = 18, $p = 0.0002$). On the other hand, the sub-acute dosing lowered TH-positive fibers and cells equally (TH-(+) fibers: >50%, $t = 5.883$, df = 27, $p < 0.0001$; TH-(+) cells: >50%, $t = 12.29$, df = 25, $p < 0.0001$). One-way ANOVA confirmed an overall treatment effect for both TH-positive fibers ($F_{[5,64]} = 14.09$, $p < 0.0001$) and Nissl-positive cells ($F_{[5,63]} = 16.50$, $p < 0.0001$), but only nuanced differences between the MPTP-treated cohorts (Figure 2g,h). Overall, the order of potency for histopathological endpoints was acute>sub-acute>chronic MPTP administration.

3.2 | Motor coordination, balance, and gait across the three MPTP models

Motor coordination and stamina were assessed with the Rotarod, but there was no difference between controls and any of the MPTP models (Figure S1). The balance beam test yielded contrasting results for sub-acute and chronic MPTP regimens (Figure 3b,c and e,f). For instance, two-way ANOVA revealed that mice in the sub-acute group were significantly faster at traversing the three different beams (main treatment effect: $F_{[1,80]} = 7.341$; $p = 0.0082$) (Figure 3b) relative to saline. By contrast, chronic MPTP treatment impaired motor coordination by increasing the latency independently of beam size ($F_{[1,52]} = 5.555$; $p = 0.0222$) (Figure 3c). No significant changes were produced by acute MPTP administration on latency to climb to the top ($F_{[1,58]} = 3.23$; $p = 0.0777$) or the number of foot slips ($F_{[1,60]} = 1.643$; $p = 0.2049$) (Figure 3a,d). Although not perturbed by the MPTP treatment, the number of foot slips did increase with the reduction of beam size confirming that mice find the smaller beams more challenging than the wider beams (See Figure S1 for normalized data). Only the quantitative assessment of gait performed 27 days post-acute MPTP treatment using the CatWalk revealed impaired run (normalized to the saline controls) and paw parameters (Figure 4). The chronic MPTP treatment increased running speed compared to control mice, whereas no effects were induced by the sub-acute MPTP regimen. One-way ANOVA of the average speed yielded an overall treatment effect ($F_{[5,65]} = 5.327$, $p = 0.0004$) with *post-hoc* test confirming the acute MPTP cohort being significantly different from the sub-acute ($p < 0.01$) and chronic ($p < 0.0001$) cohorts, while no overall changes were seen for the base of support (see Table 1, $F_{[5,65]} = 2.296$, $p = 0.0553$). In contrast, the acute MPTP regimen alone affected several parameters, including a significant lowering of the running speed ($t = 2.614$, df = 20, $p = 0.016$), and increased the base of support (see Table 1, $t = 2.356$, df = 20, $p = 0.029$ - Figure 4a,b). In depth analysis of paw parameters for the acutely treated cohort showed that swing speed ($F_{[1,80]} = 12.66$, $p = 0.0006$), stride length ($F_{[1,80]} = 9.751$, $p = 0.0025$), stance ($F_{[1,80]} = 6.23$, $p = 0.014$), step cycle ($F_{[1,80]} = 5.63$, $p = 0.02$), and duty cycle ($F_{[1,80]} = 12.48$, $p = 0.0007$) were consistently impaired (Figure 4c–g). These data are in line with the strongest lowering of DA content observed in the acute model. None of these parameters were affected by sub-acute or chronic MPTP regimes.

3.3 | Habituation to novel environment and total ambulatory activity in the home cage

The habituation locomotor curves pertaining to the three models fit a one-phase non-linear decay function with significant differences attained for the acute and sub-acute model. By contrast, the chronic model did not reveal any substantial differences in the habituation to novel environment (Figure 5 and Table 2). We next asked whether the habituation behavior (reduction of ambulatory activity) was different for the three MPTP models compared with their respective controls. A significant difference was confirmed for both acute and sub-acute MPTP cohorts, but not in the chronic model (Figure 5a,d,g; Table 2). Circadian and ultradian rhythmicity was evaluated in the PhenoTyper home cages by recording ambulation over 4 days/nights from recording day 3 (Monday) until day 7 (Thursday) (Figure 5b,e,f). Overall, locomotor activity binned over 2 h showed the typical circadian rhythm

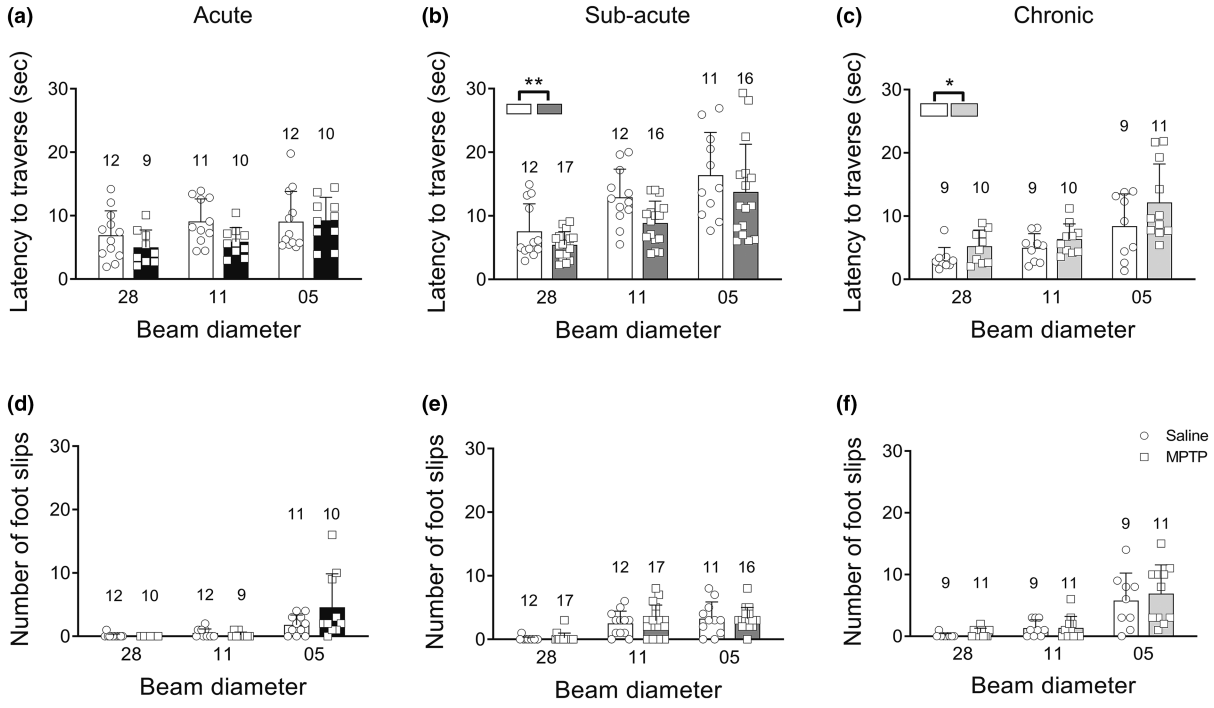

FIGURE 3 Balance across the three different MPTP models. (a–c) Latency to traverse 50 cm long balance beams of three diameters, 05, 11, and 28 mm in the three MPTP regimens differed considerably. (a) Acute dosing had no effect of balance beam performance. (b) Mice treated with the sub-acute MPTP performed significantly better with no effect on number of foot slips. (c) Chronic MPTP significantly impaired the ability to traverse the beams but had no effect on number of foot slips. (d–f) The number of foot slips was not affected by the MPTP treatments but increased with smaller beam diameter. Balance beam test data were reported as mean, SD and treatment effects were analyzed by two-way ANOVA with treatment as between and beam size as within subject factors, followed by two-tailed student *t*-tests. $^{*}p<0.05$, $^{**}p<0.01$. Acute model, saline $n = 12$, MPTP $n = 10$; sub-acute model, saline $n = 12$, MPTP $n = 17$; chronic model, saline $n = 9$, MPTP $n = 11$. n = number of mice. The data set pertaining to the sub-acute regimen for diameter five present one missing data point in both the saline and MPTP group, respectively, due to the animal not being able to complete the task. Actual sample size after outliers exclusion is stated on top of each bar chart.

with strongly increased horizontal activity during the night *versus* light hours. All groups showed multi-phasic activity patterns with activity peaks early and late during darkness (de Visser et al., 2007). Only the sub-acute MPTP treated mice showed a significant increase in locomotor activity ($F_{[11431]} = 16.50$; $p<0.0001$) (Figure 5e), which was most prevalent during darkness hours (i.e. active phase). Independent of locomotor activity, enhanced water consumption and food intake were consistently observed for all three MPTP models over the 7 days of recording (Figure 5e,f,i; all F's > 3.9, p's < 0.05).

3.4 | Anhedonia, anxiety-like behavior, and cognition in MPTP models of Parkinson's disease

The use of the LDB apparatus developed by Crawley and Goodwin (Crawley & Goodwin, 1980) revealed a significant reduction in the latency to first enter the dark compartment (Figure 6a) solely in the sub-acute model ($t = 3.676$, df = 27, $p = 0.001$) likely to result from generalized hyperactivity (distance covered $t = 1.968$, df = 27, $p = 0.0297$, data not shown, average speed was unchanged). Furthermore, time spent in the light compartment was altered ($F_{[5,70]} = 2.67$; $p<0.0297$) with a significant reduction in the sub-acute (saline, $p = 0.007$; MPTP, $p = 0.045$) and chronic cohorts (saline, $p = 0.0081$; MPTP, $p = 0.0044$) relative to the 50% chance level (Figure 6b). The sucrose preference test yielded a significantly higher consumption of sucrose compared with the 50% chance level in all MPTP treated cohorts (acute, $p = 0.0012$; sub-acute, $p = 0.022$; chronic, $p<0.0001$); however, significant differences against control groups were not observed (Figure 6c). The olfactory discrimination test was implemented to seek anxiety like behavior based on two assumptions: (i) MPTP does not induce olfactory alteration in mice (Kurtenbach et al., 2013); (ii) healthy mice tend to spend significantly more time in the familiar compartment due to their natural aversion toward a novel environment (Kurtenbach et al., 2013; Prediger et al., 2006). Nonetheless, the latter assumption was not met based on the distribution of the saline cohorts (Figure 6d). The sub-acute ($p<0.0001$) and chronic MPTP treated mice ($p = 0.0216$) were the sole cohorts spending significantly more time in the familiar zone compared with the 50% chance level (Figure 6d). A significant MPTP effect was observed on total distance moved ($F_{[5,70]} = 10.36$; $p<0.0001$) with post-hoc analyses revealing significant differences among the three MPTP treated cohorts. Moreover, pairwise comparison revealed a significant increase in activity in the sub-acute MPTP cohort compared with the control group ($t = 3.842$, df = 27,

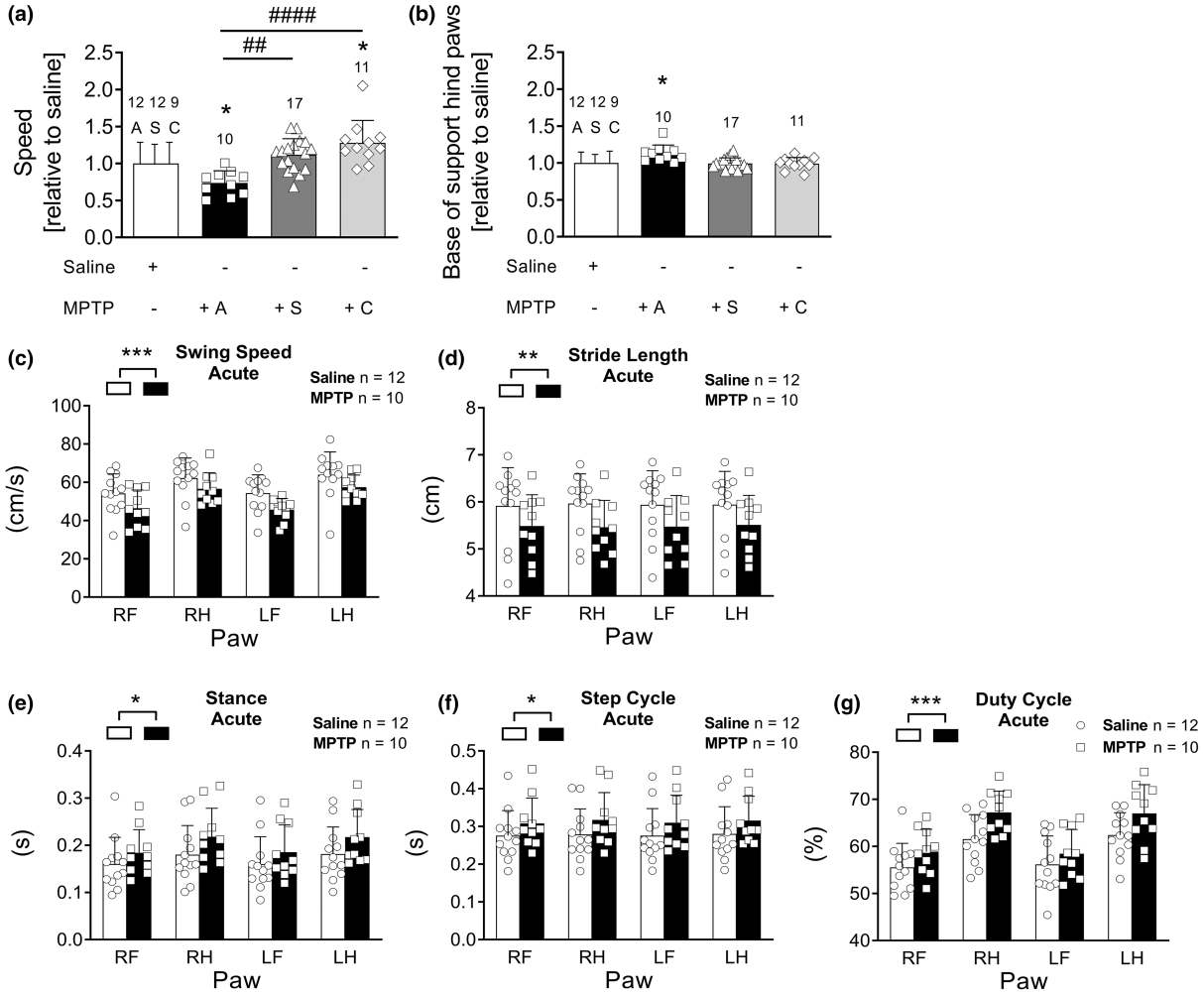

FIGURE 4 Quantitative assessment of gait changes. (a) The overall running speed was reduced by the acute MPTP administration compared with the control; chronic MPTP injections increased speed. (b) Base of support defined as average distance between the hind paws expressed in centimeters (cm). Acute MPTP increased base of support. Speed and base of support data were reported as mean, SD and normalized to saline groups. Saline groups were condensed in one bar chart with individual SD bars (A = acute, saline $n = 12$, MPTP $n = 10$; S = sub-acute, saline $n = 12$, MPTP $n = 17$; C = chronic, saline $n = 9$, MPTP $n = 11$. n = number of mice). Differences between MPTP groups were assessed with one-way ANOVA. (c–g) Gait analysis in the acute model suggests a severe impairment in multiple dynamic and static gait parameters. Stance is the time in seconds (s) a paw is in contact with the ground. Step cycle pertains to the time between two consecutive contacts of the same paw with the ground. The duty cycle expresses the stance as percentage of the step cycle. The swing speed in the speed at which a paw moves between two consecutive contacts with the glass platform while stride length is the distance between two consecutive contact of the same paw with the glass platform. Gait measurements from acute MPTP treatment are presented for each individual paw as mean, SD and analyzed with a two-way ANOVA under null hypothesis that treatment affected gait (RF = right front, LF = left front, RH = right hind, LH = left hind) were equally affected by acute MPTP, but no other administration regime followed by Bonferroni post-hoc test $^{*}p < 0.05$, $^{**}p < 0.01$, $^{***}p < 0.001$. MPTP cohorts were compared using one-way ANOVA followed by Bonferroni post-hoc tests where applicable to seek for differences among MPTP cohorts only $\#\#p < 0.01$ $\#\#\#\#p < 0.0001$. Actual sample size after outliers exclusion is stated in each bar chart.

$p = 0.0007$) and a decrease in the chronic MPTP cohort ($t = 2.595$, df = 18, $p = 0.0183$) (Figure 6e). The 16-hole Barnes maze did not reveal any learning or memory impairments across the three models (Figure 6f–h). The path length proxy was not altered in the sub-acute cohorts confirming the transitory nature of the hyperactivity phenotype observed in behavioral tests administered at earlier time points (Figures 1d and 6g). In addition, the test duration for sub-acute MPTP cohort was significantly increased (two-way ANOVA: $F_{[1216]} = 10.49$, $p < 0.0014$, data not shown) suggesting freezing behavior with respect to the augmented velocity Figure 6g. No meaningful changes were observed for path length, velocity and test duration for the acute and chronic model (Figure 6f,h).

3.5 | Correlations of nigrostriatal lesion endpoints across the models and gait: correlations in the acute model only

To validate the accuracy of the nigrostriatal lesion assessment, correlations were probed across the three lesion endpoints (Figure 7).

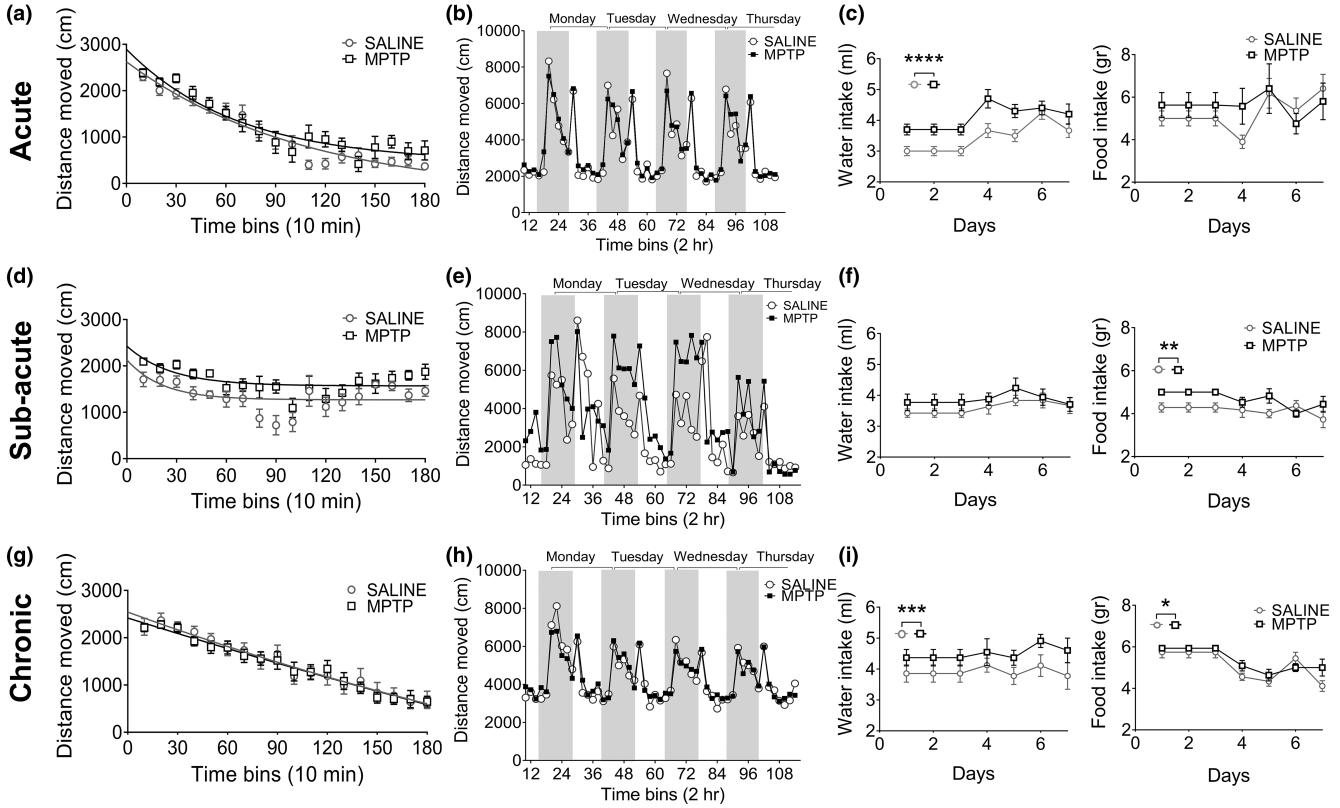

FIGURE 5 Habituation to novel environment and circadian locomotor activity recorded in PhenoTyper home cages. The locomotor readouts obtained within the first 3 h from the acute (a), sub-acute (d) and chronic (g) cohorts revealed a decay fitting the one phase non-linear regression function described as $Y = (Y_0 - \text{Plateau}) \bullet e^{(-K \bullet X)} + \text{Plateau}$. The sub-acute (e) MPTP treatment significantly affected the locomotor activity over a period of 4 days ($p < 0.0001$) highlighting the presence of hyperactivity. No changes in gross locomotor activity were observed in acute and chronic regimen (b, h). Circadian and ultradian rhythms were normal in all MPTP cohorts. Water and food intake recorded over a period of 7 days across the three models (c, f and i). Data are presented as mean (b, e and h) or mean, SD Data were analyzed using repeated measure two-way ANOVA followed by Bonferroni post hoc test for single data point differences; $^{*}p < 0.05$, $^{**}p < 0.01$, $^{***}p < 0.001$, $^{****}p < 0.0001$. Acute model, saline $n = 12$, MPTP $n = 10$; sub-acute model, saline $n = 12$, MPTP $n = 17$; chronic model, saline $n = 9$, MPTP $n = 11$. n = number of mice.

TABLE 2 Summary of the statistical analysis for the habituation to novel environment implemented across the MPTP models

	Non-linear fit, exponential one-phase decay function					Two-way ANOVA
Treatment groups	***Y0***	**Plateau**	**K**	**Tau**	***F (DFn, DFd); p***	**Treatment effect**
Acute					4.057 (3386); 0.0074	$F_{(1,360)} = 9.583$; $p = 0.0021$ Int: n.s.
Saline ($n = 12$)	2624 ± 140.1	−257.9 ± 345.3	0.009 ± 0.002	108.1		
MPTP ($n = 10$)	2894 ± 204.6	454.2 ± 187.0	0.014 ± 0.004	66.93		
Sub-acute					10.80 (1479); 0.0011	$F_{(1,486)} = 35.83$; $p < 0.0001$ Int: n.s.
Saline ($n = 12$)	2131 ± 413.7	1269 ± 57.19	0.046 ± 0.028	21.45		
MPTP ($n = 17$)	2428 ± 314.6	1570 ± 58.13	0.038 ± 0.019	26.49		
Chronic					0.28 (3352); 0.8393	$F_{(1,324)} = 0.6764$; $p = 0.4114$ Int: n.s.
Saline ($n = 9$)	2543	−3766	0.002	489.5		
MPTP ($n = 11$)	2418	−9455	0.001	1073		

Note: The habituation to novel environment generated readouts fitting the non-linear exponential one-phase decay function (see Figure 5 legend for details). Parameters and constants are reported in the table. Data were generated during the first 3 h of home cage observation and represent horizontal locomotor activity averaged into 10-min time bins. Significant differences were sought by comparison of the fits and by two-way analysis of variance. Values are reported as mean, S.E. Int. = interaction, n.s. = non significant. n = number of animals.

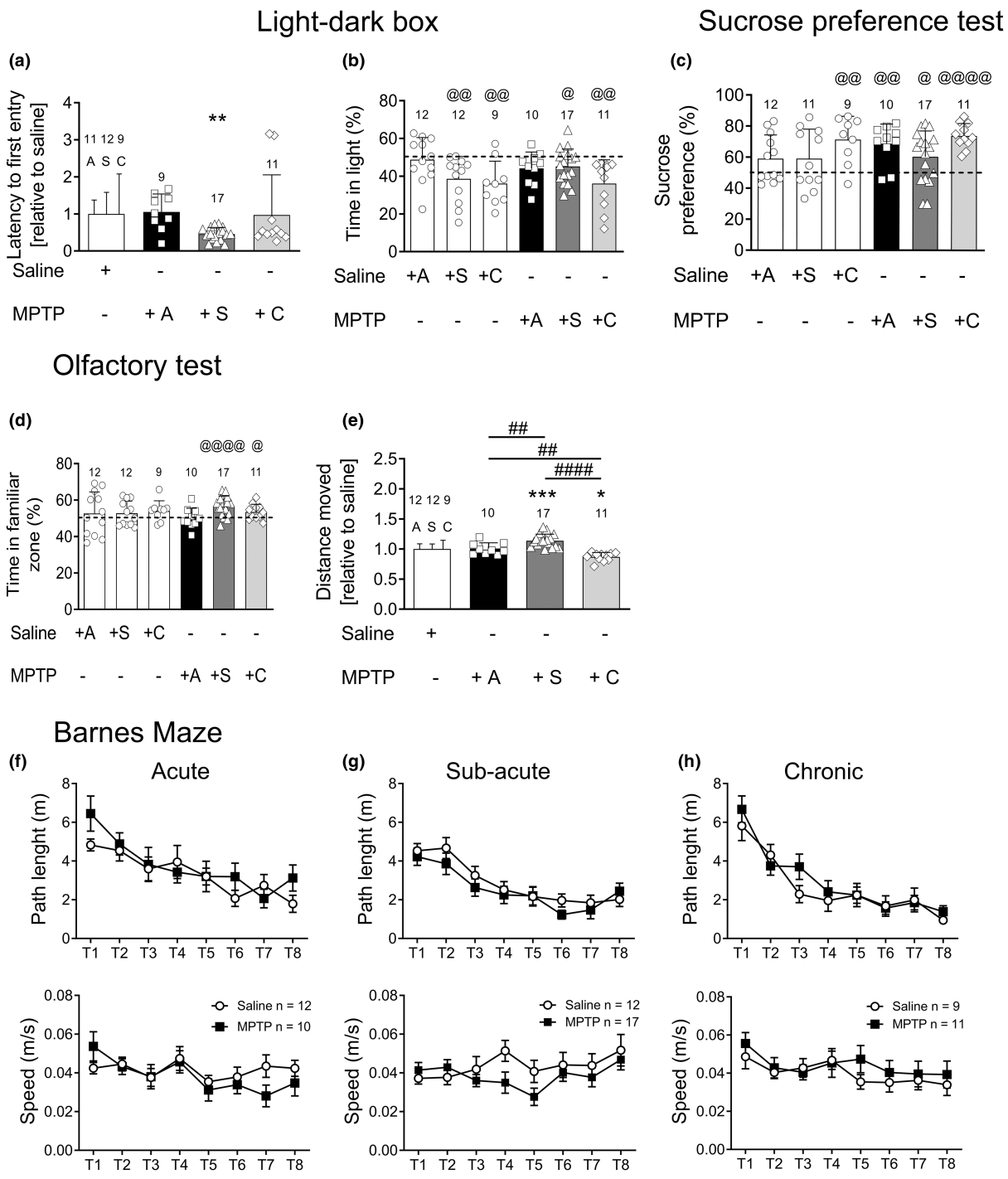

FIGURE 6 Light–dark box (LDB) test, sucrose preference test, olfactory discrimination test and Barnes maze. (a) Latency to first enter the dark compartment of the LDB apparatus and (b) time spend in the light compartment reported as percentage of the total test duration, $^{*}p<0.05$, $^{**}p<0.01$. (c) Sucrose preference measured over a period of 48 h and expressed as percentage of total fluid consumption, $@p<0.05$, $@@p<0.01$, $@@@@p<0.0001$. (d, e) Time in familiar zone expressed as percentage of total test duration and overall locomotor activity; values were normalized to saline and saline groups condensed in one bar chart. Visuospatial memory test revealed no treatment effect. Graphs f–h show the average distance covered by the mice prior entering the target hole as well as the average speed as indicator of motor function over a period of 4 days. Differences between saline and MPTP-treated groups were sought using repeated measures two-way ANOVA. Data presented are expressed as mean, SD (A = acute, saline $n = 12$, MPTP $n = 10$; S = Sub-acute, saline $n = 12$, MPTP $n = 17$; C = chronic, saline $n = 9$, MPTP $n = 11$. n = number of mice). MPTP cohorts were compared using one-way ANOVA followed by Bonferroni post-hoc tests where applicable to seek for differences among MPTP cohorts only $\#\#p<0.01$ $\#\#\#\#p<0.0001$. Actual sample size after outliers exclusion is stated on top of each bar chart and line graph.

All correlations across the three MPTP model (9 in total) were positive and yielded statistically significant p values with histological endpoints being highly interdependent across the three models, (acute: $r^2 = 0.3767$, $p = 0.0031$; sub-acute: $r^2 = 0.5398$, $p < 0.0001$; chronic: 0.4237, $p < 0.0026$. Figure 7g–i). Being the acute model most severely affected, striatal DA content correlated well with TH-positive fibers and TH-positive cells in the SNpc (Figure 7 A $r^2 = 0.5079$, $p = 0.0002$ and D $r^2 = 0.3554$, $p = 0.0043$) but less so for sub-acute and chronic models.

Table 4 summarizes the significant behavioral changes across the three different regimens providing a rationale for the correlation analyses summarized in Table 3. Reduced DA content in the STR is the result of a dysfunctional nigrostriatal system where DA neurons succumbed to the MPTP toxicity. Consequently, Pearson's correlation analysis was used to seek out potential relationships between a dysfunctional nigrostriatal system and behavioral endpoints. Overall, the striatal DA content poorly correlates with behavioral performance. Sub-acute MPTP treatment revealed an association between DA levels and only four behavioral parameters: latency to enter the dark compartment (in the LDB, $p = 0.0041$), latency to traverse the 11 mm balance beam ($p = 0.0023$), distance moved in the olfactory test ($p = 0.0373$), and duty cycle pertaining to the front paws generated from gait analysis ($p = 0.0463$) (Table 3). Two of the worsened gait parameters observed in the acute model correlated positively with the level TH-positive fibers; speed ($p = 0.0407$) and stride length (front $p = 0.04701$ and hind $p = 0.0493$). Equally, positive correlation with TH cell count in the SNpc was observed (speed: $p = 0.0002$, stride length: front $p = 0.0669$ and hind $p = 0.0457$). By contrast, for the paw parameters stance ($p = 0.0281$), duty cycle ($p = 0.0095$), and step cycle ($p = 0.0445$) a negatively correlation with the TH cells count is highlighted in Table 3. Latency to traverse the 11 mm balance beam also correlated with striatal DA content in the acute cohort (Table 3, $p = 0.0059$). In chronically treated MPTP animals, the balance beam performance did not correlate with either DA striatal content or with density of TH striatal fibers and cells in the SNpc (Table 3). On the other hand, in sub-acute MPTP treated animals, the lesion size measured correlated consistently with the motor phenotype observed in the LDB test (distance covered *versus*

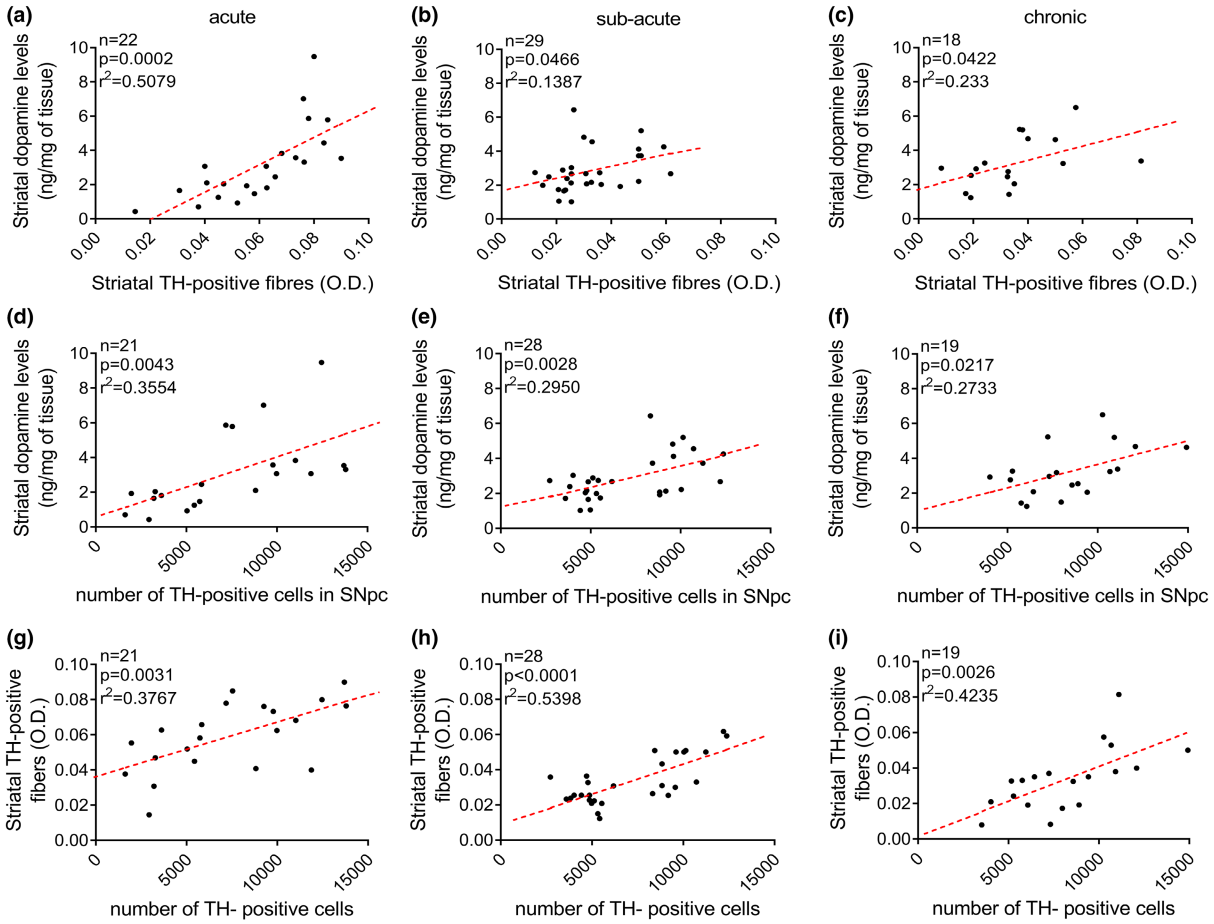

FIGURE 7 Graphical display of the relationship between biochemical and histological endpoints at striatal and nigral (SNpc) level. Pearson's correlation analyses revealed a significant link between striatal DA level and histological endpoints in acute regimen at striatal (a) and SNpc level (d). Number of TH-positive cells and fibers also robustly correlated with DA content in sub-acute animal model (b and e). The chronic model showed only a weakly significant correlation between the two variables (c and f). (g–i) A stronger significant correlation was highlighted by Pearson's correlation analysis between the two histological endpoints in the *striatum* and SNpc, respectively. Total sample size is stated in each scatter plot after outliers removal. n = number of mice

TABLE 3 Summary of Pearson's correlation analysis of significantly affected behavioral paradigms versus striatal dopamine (DA) levels, striatal TH-positive fibers and nigral TH-positive cell numbers

Behavioral test/*parameter considered*	Striatal DA content (ng/mg of tissue)			Striatal TH fibers (O.D.)			Nigral TH-positive cell number		
	Acute	Sub-acute	Chronic	Acute	Sub-acute	Chronic	Acute	Sub-acute	Chronic
Light–dark box									
Time in light—%	n.s.	n.s.	n.s.	n.s.	n.s.	n.s.	n.s.	0.1752 (−), p = 0.0266	n.s.
Latency to dark—sec	n.s.	0.267(+), p = 0.0041	n.s.	n.s.	0.1465 (+), p = 0.0405	n.s.	n.s.	0.1630 (+), p = 0.0331	n.s.
Path length in light—m	n.s.	n.s.	n.s.	n.s.	0.1409 (−), p = 0.0448	n.s.	n.s.	0.1743 (−), p = 0.0271	n.s.
Balance beam test									
Latency to traverse 5 mm—sec	n.s.	n.s.	n.s.	n.s.	n.s.	n.s.	n.s.	n.s.	n.s.
Latency to traverse 11 mm—sec	0.3221 (+), p = 0.0059	0.296(+), p = 0.0023	n.s.	0.1943 (+), p = 0.0401	n.s.	n.s.	n.s.	n.s.	n.s.
Latency to traverse 28 mm—sec	n.s.	n.s.	n.s.	n.s.	n.s.	n.s.	n.s.	n.s.	n.s.
PhenoTyper									
Day activity—m	n.s.	n.s.	n.s.	n.s.	n.s.	n.s.	n.s.	n.s.	n.s.
Night activity—m	n.s.	n.s.	n.s.	n.s.	n.s.	n.s.	n.s.	n.s.	n.s.
Olfactory discrimination test									
Path lenght – cm	n.s.	0.1509 (−), p = 0.0373	n.s.	n.s.	0.2353 (−), p = 0.0076	n.s.	n.s.	0.3124 (−), p = 0.002	n.s.
Latency to first entry—sec	n.s.	n.s.	n.s.	n.s.	0.2066 (+), p = 0.0132	n.s.	n.s.	0.2612 (+), p = 0.0054	n.s.
CatWalk									
Speed—cm/sec	n.s.	n.s.	n.s.	0.1932 (+), p = 0.0406	n.s.	n.s.	0.529(+), p = 0.0002	n.s.	n.s.
Swing speed front paws—cm/sec	0.1817 (+), p = 0.0479	n.s.	n.s.	0.3241(+), p = 0.0057	n.s.	n.s.	0.3661 (+), p = 0.0037	n.s.	n.s.
Swing speed hind paws—cm/sec	n.s.	n.s.	n.s.	n.s.	n.s.	n.s.	0.2612 (+), p = 0.0179	n.s.	n.s.
Stride length front paws—cm	n.s.	n.s.	n.s.	0.1830(+), p = 0.0471	n.s.	n.s.	n.s.	n.s.	n.s.
Stride length hind paws—cm	n.s.	n.s.	n.s.	0.1796 (+), p = 0.0493	n.s.	n.s.	0.1940 (+), p = 0.0457	n.s.	n.s.
Stance hind paws—sec	n.s.	n.s.	n.s.	n.s.	n.s.	n.s.	0.2292 (−), p = 0.0281	n.s.	n.s.
Duty cycle hind paws—%	n.s.	n.s.	n.s.	0.2245 (−), p = 0.0259	n.s.	n.s.	0.3047 (−), p = 0.0095	n.s.	n.s.
Step cycle hind paws—sec	n.s.	n.s.	n.s.	n.s.	n.s.	n.s.	0.1959 (−), p = 0.0445	n.s.	n.s.

Note: For statistically significant correlation reportedly r^2 values are followed by p values; n.s. = non-significant; the symbols (+) and (−) indicates whether the correlation is positive or negative. Acute, saline n = 12, MPTP n = 10; sub-acute, saline n = 12, MPTP n = 17; chronic, saline n = 9, MPTP n = 11. n = number of mice.

TABLE 4 Summary of behavioral changes induced by MPTP regimens sorted by paradigm

Behavioral test/*parameter considered*	MPTP regimens		
	Acute	Sub-acute	Chronic
Light–dark box			
Time in light compartment—%	n.s.	n.s.	n.s.
Latency to dark compartment—sec.	n.s.	**↓	n.s.
Distance covered in light compartment—m	n.s.	*↑	n.s.
Rotarod			
Latency to fall—sec.	n.s.	n.s.	n.s.
Balance beam test			
Latency to traverse—sec.	n.s.	*↓	**↑
PhenoTyper			
Habituation to novel environment – m	**↑	****↑	n.s.
Activity—m	n.s.	****↑	n.s.
Food intake—gr.	n.s.	**↑	*↑
Water intake—ml.	****↑	n.s.	***↑
Sucrose preference test %	n.s.	n.s.	n.s.
Olfactory discrimination test			
Time in familiar zone – %	n.s.	n.s.	n.s.
Distance covered—cm	n.s.	***↑	*↓
Latency to first entry—sec.	n.s.	****↓	n.s.
Total transitions—n	n.s.	n.s.	n.s.
CatWalk			
Speed—cm/sec.	*↓	n.s.	*↑
Cadence—steps/sec.	n.s.	n.s.	n.s.
Base of support hind—cm	*↑	n.s.	n.s.
Overall swing speed—cm/sec.	***↓	*↑	**↑
Overall stride length—cm	**↓	n.s.	n.s.
Overall stance—sec.	*↑	n.s.	**↓
Overall duty cycle—%	***↑	n.s.	n.s.
Step cycle—sec.	*↑	*↓	****↓
Barnes maze			
Path length—m	n.s.	n.s.	n.s.
Speed—m/sec	n.s.	n.s.	n.s.

Note: Statistical comparison to healthy control animals was made using the two-tailed student *t*-test. n.s. = non-significant; *$p < 0.05$, **$p < 0.01$, ***$p < 0.001$, ****$p < 0.0001$; ↑ = increased readout compared with saline control mice, ↓ = decreased readouts compared with saline control mice. m = meter, cm = centimeter, gr = gram, ml = milliliter, sec = second, *n* = number. Number of animals in each group. Acute, saline $n = 12$, MPTP $n = 10$; sub-acute, saline $n = 12$, MPTP $n = 17$; chronic, saline $n = 9$, MPTP $n = 11$.

TH fibers, $p = 0.0448$ and *versus* TH cells, $p = 0.0271$), and in the olfactory discrimination test (distance covered *versus* TH fibers, $p = 0.0076$ and *versus* TH cells, $p = 0.002$). Similarly, the latency to first enter the familiar zone and the distance covered in the olfactory discrimination test correlated with TH fibers (latency $p = 0.0405$, distance $p = 0.0448$) and TH cell numbers (latency $p = 0.0331$, distance $p = 0.0271$). Taken together our results suggest that the acute model seems to generate the most reliable nigrostriatal damage resulting in gate changes proportional to the lesion extent. Balance impairment was observed in the chronic model while the sub-acute mouse model displayed a behavioral phenotype poorly translatable in MS and NMS affecting PD patients. In relation to non-motor paradigms, habituation to a novel environment seems to be slowed down in the acute and chronic model while water and food consumption seems to be increased by each MPTP regimen.

4 | DISCUSSION

Here, we assessed in a direct side-by-side comparison the validity of three frequently used pharmacological MPTP mouse models of PD both in terms of core pathology of the nigrostriatal system and the movement impairments. Our data reveal significant differences in terms of size and severity of pathological lesions and behavioral outcomes (Tables 3 and 4). Quantitative indicators showed consistent gait deficits in the acute mouse model while balance and motor coordination were altered in MPTP chronically treated mice. On the other hand, habituation to a novel environment was different with significant alterations attained in the acute and sub-acute models only. Besides, we report for the first time an overall increase in water and/or food intake across all three MPTP models. Correlation analysis highlighted a poor relationship between the levels of striatal DA and the behavioral performance for MS and NMS in any MPTP models. Nevertheless, a positive correlation confirmed that the acutely MPTP-induced gait deficits were associated with dopaminergic lesion of the nigrostriatal system, but both sub-acute and chronic administrations failed to yield such phenotypes. Significant reductions in DA content were observed across the three different MPTP models with the greatest reduction of ≈ 68% in the acute model against a lowering of ≈ 44–50% attained in the sub-acute and chronic regimens. These findings are in line with MPTP mouse model guidelines released by Jackson-Lewis and Przedborski where striatal levels of DA are shown to be depleted by 40–50% in the acute and sub-acute model (Jackson-Lewis and Przedborski, 2007). On the other hand, the lesion extent observed in the chronic model is not entirely aligned with the literature; in fact, Bezard and colleagues reported a reduction of 70% of TH-positive neurons in the SNpc *versus* our observation of 41% (Bezard et al., 1997a; Bezard et al., 1997b). In light of these discrepancies, it is important to bear in mind that several mouse strains present different sensitivity to MPTP yielding therefore inconsistent results in relation to the lesion size. For instance, C57BL/6J strain is the most sensitive while BALB/c mice are less vulnerable to the MPTP neurotoxicity (Filipov et al., 2009). For instance, the differences between our findings in the chronic model and the results reported in literature could be due to the OF1 mouse strain used by Bezard and colleagues (Bezard et al., 1997a; Bezard et al., 1997b).

Reduced striatal content of the DA metabolites DOPAC and HVA is the functional result of a lesioned nigrostriatal system while the ratio of DOPAC/DA and HVA/DA highlight changes in the turnover of DA which was consistently increased in the sub-acute model, partially increased in the acute model but not altered in the chronic model. These data could suggest that the depletion of DA in both acute and sub-acute models was severe enough to induce catabolic changes. By contrast, the reduction of DA in the chronic model was less severe and unlikely to influence the metabolic turnover of DA. Theory holds that levels of DOPAC are directly affected by the MPTP toxicity since the membrane bound catechol-o-methyl-transferase (COMT) is located within dopaminergic neurons, while HVA levels are indirectly affected since the MAO_B enzyme (which metabolizes DOPAC) is more abundant in glial cells (Chen et al., 2011; Tong et al., 2013). This, however, was not reproduced in our investigation, since correlation analyses of DOPAC versus DA and HVA versus DA content showed similar coefficients (data not shown) in all models.

Motor deficits were most consistently registered using the Catwalk and the balance beam apparatus. Such observations revealed that gait features of acutely treated mice correlated with both density of TH-positive fibers and with the number of TH-positive cells. By contrast, the balance impairment observed in the chronic model was not supported by a significant correlation with the striatal content of DA. Disruption in balance and coordination might arise from the widespread MPTP toxicity which in turn causes a serious lowering in proprioceptive responsiveness at the peripheral level in monkeys with consequent impairment of CNS feedback circuitry in the cortical motor area and in the thalamus (Escola et al., 2002; Pessiglione et al., 2005; Ribeiro et al., 2011). Similarly affected by the MPTP is the vestibular system, which is involved in balance and movement control (Wu et al., 2016) while MPTP effects on the proprioceptive systems remain to be examined given that previous work has reported deficits in balance only for the sub-acute, but not the acute model (Anandhan et al., 2010; Prema et al., 2015). In this specific case, authors have used male C57BL/6 mice but did not report the age of the mice at the time of the MPTP administration and behavioral testing was carried out only 7 days post MPTP administration.

As for impairments of gait related proxies, Wang and colleagues (Wang et al., 2012) were the first to provide a detailed analysis of quantitative gait parameters in the sub-acute MPTP mouse model using the catwalk. They showed gait deficits correlating with lesion extent at nigral level, detected at 7 and 21 days post-MPTP administration. Our findings contrast with their data in that hardly any parameter of gait was abnormal in our sub-acute cohort, even though similar reductions in TH-positive cell counts were reported in both experiments. Method differences between studies including bigger cohort sizes and, in our case, a longer time window for the establishment of the lesion might explain the variation in outcome. Moreover, the effectiveness of our behavioral protocol was confirmed by inclusion of the acute MPTP model, which caused not only greater lesion sizes but also stronger effects on gait. This is among the most robust correlations found in this study and in line with the number of foot slips observed in the balanced beam test (see Figure 3 and Figure S1). Overall, we consider the acute MPTP model a suitable platform for the screening of neuroprotective compounds since it allows to asses gain of function at gait level and lesion extent of the nigrostriatal pathway. Nonetheless, experimenters must take into account the acute insult induced by MPTP and the short time course of the nigrostriatal lesion, which often require pre-medication with the test compound. Such shortcoming undermines the translational relevance of such a model in light of the slow and progressive nature of PD. Intuitively, the chronic model might provide the best kinetics in terms of dopaminergic lesion of the nigrostriatal pathway, allowing a large margin for therapeutic interventions and the yield of a more translatable outcome. Among the three regimens, the sub-acute model is the mostly used in spite of its behavioral inconsistencies. The model was characterized by increased locomotor activity and generalized hyperactivity observed in various tests such as a novel environment, the home cage monitoring, the LDB, and the olfactory discrimination test. Interestingly, such conditions are both prodromal to and a co-morbidity of PD with a high prevalence (Curtin et al., 2018; Yang et al., 2018). Only one report has so far highlighted hyperactivity in C57BL6/J mice following MPTP treatment (Wang et al., 2013), and it is surmised due to the lower DA levels in the cortex and neocortex (Luchtman et al., 2009) or altered mesocortical norepinephrine levels (Espejo & Miñano, 2001).

Signs of hyperactivity as reported by Wang and colleagues showed amelioration following electrostimulation of the limbs (Wang et al., 2013) while Zhang's laboratory reported improved motor performance on the rotarod test associated with hyperactivity (Zhang et al., 2017). Hyperactivity may be a compensatory response following nigrostriatal lesions (Zhang et al., 2017) although the underlying mechanism remains elusive. In the present study, we hypothesize that hyperactivity has a major impact on the overall single-phase decay habituation functions to the novel environment and overall activity (Phenotyper) making it difficult to draw conclusions on the presence of associative learning deficits. While the origin is unclear, this hyperactivity is parsimoniously explained by an overflow of DA and persistent activation of hypersensitized receptors. The phenotype is somewhat reminiscent to treatment of mice with amphetamine/apomorphine and indicative of a heightening (not lowering) of dopaminergic tone potentially explaining the reported higher DA turnover in the sub-acute model (Bagga et al., 2015). A contending hypothesis would suggest that this hyperactivity is unrelated to dopaminergic changes since both acute and chronic MPTP regimes also cause severe loss of TH in the *nigra* cells and in STR but were without gross changes in activity (Figure 2; Table 4 and Table S2). Other studies suggest that the increased locomotion could be orchestrated by the noradrenergic neurons in the mesocortical regions (Espejo & Miñano, 2001).

Despite robust signs of short-term memory deficits in some PD patients (Fallon et al., 2019; Zokaei et al., 2020), previous attempts to back-translate this finding have also met with inconsistent results (Volkow et al., 2011). Short term memory deficits in negatively reinforced avoidance tasks were however consistently reported in mice

infused with an intranasal dose of MPTP (Anderson et al., 2007; Matheus et al., 2012) and various systemic administration regimes (Han et al., 2021; Kim et al., 2021; Sampaio et al., 2018). Interestingly, impaired habituation has been observed in dopamine transporter (DAT) knock out mice (Zhuang et al., 2001) while faster habituation in DAT overexpressors (Spielewoy et al., 2000) suggesting that DAT function could have been altered in the acute and sub-acute model which presented with altered habituation to a novel environment. Conversely, the use of the Barnes maze apparatus did not reveal any significant changes regarding the visuo-spatial learning and working memory functions. Throughout the last two decades, the detection of memory deficits in the MPTP mouse model has proven challenging and studies using elevated plus-maze and Morris water maze (Zhang et al., 2018) have reported contrasting results. Zhang and colleagues have used a slightly modified sub-acute regimen extended from 5 to 7 days while mice were of the same strain, sex and age (Zhang et al., 2018).

The circadian rhythm was also not disrupted in any of the three mouse models, and this is consistent with previous work (Liu et al., 2020). Increased water and food intake observed in the acute, sub-acute, and chronic models has not been reported before. However, given the crucial role of DA in reward sensitivity and in the regulation of food intake (Thanarajah et al., 2019) this result is counterintuitive and might arise from compensatory mechanism taking place in the mesocortical dopaminergic pathway (Luchtman et al., 2009). Furthermore, a prudent explanation for the sub-acute model is the observed hyperactivity (for a discussion of this phenotype, see above) and subsequent increase in energy expenditure, which may drive the increase in food intake. However, such an interpretation does not apply to acute and chronic MPTP regimen, in which we do not report any change in activity levels, yet water consumption was increased. Furthermore, body weights were monitored across the three different models and revealed no differences between MPTP and control groups (see Figure S2). Consistently, MPTP does not impact the mouse body weight (Zhang et al., 2015, 2017); therefore, the misalignment between food intake and macronutrients absorption in the gut could explain the lack of change in body weight. This could be due to perturbed gut microbiota impinging on the concentration of short fatty acids which are known to affect the metabolism (Zhou et al., 2019). In addition, Liu et al. (2021) have reported reduced expression of tight-junctions, villus height and mucosal thickness as signs of intestinal inflammation following sub-acute MPTP intoxication (Liu et al., 2021). Such findings may potentially explain the enhanced food intake but lack of weight gain observed in our models.

Up until now, studies exploring anxiety-like traits in MPTP mouse models have been inconclusive (Shin et al., 2014) or requiring a challenge such as emotional stressors (confrontational housing (Mitsumoto et al., 2019) or chronic mild stress (Janakiraman et al., 2016)). The LDB, as reported elsewhere for the elevated plus maze (Sedelis et al., 2000), did not reveal any anxiety-like phenotype in any model, (Vučković et al., 2008); similarly, the sucrose preference test did not disclose any anhedonic behavior in MPTP treated mice compared with control groups. In previous work, the sub-acute MPTP regimen induced anhedonia in only 66% of subjects (Zhang et al., 2015) while Schamne and colleagues have highlighted increased susceptibility to anhedonic- and depressive-like symptoms in female C57BL/6 mice treated with MPTP intranasally (Schamne et al., 2018). We take this as evidence that the reduction of DA in the brain after MPTP exposure (about 65%) was not sufficient to affect emotional and depression related phenotypes or that brain regions other than SNpc or STR exert control of depressive symptoms (Tye et al., 2013).

Overall, the pathology among the models showed significant differences, but the behavioral proxies were not aligned with the lesion extend. The most robust outcome was the hyperactivity induced by sub-acute treatment, which was observed in multiple behavioral tests. By contrast, the acute model showed the most significant alterations in gait parameters followed by balance impairment in the chronic model. These data suggest that despite great lesion sizes among the models, extra-nigrostriatal degeneration such as the ventral tegmental area and the *locus coeruleus* should be taken into account in future experiments for a more in-depth characterization of these models. In addition, to shed light on the relationship between dopaminergic lesion and behavioral changes identified in the present study L-DOPA challenge across the three regimes will be paramount. Moreover, a similar approach might be required in stratified human cohorts were certain predominant forms of PD could be associated to specific neurodegenerative and histopathological patterns.

AUTHOR CONTRIBUTIONS

Matteo Santoro: wrote the manuscript and conducted all the in-vivo animal work, behavioral assessment and post-mortem histology evaluation of lesion extent. Data analysis and data processing. Paola Fadda: HPLC neurochemical assessment and data processing. Katie J. Klephan: CatWalk XT (Noldus) gait data extraction and processing. Gait data analysis across the three MPTP mouse models. Claire Hull: manuscript revision and writing. Peter Teismann: owner of the MPTP mouse model animal license and person in charge of overseeing the MPTP handling and injection in mice C57BL6J. Bettina Platt: study design and manuscript revision including statistical analysis revision. Gernot Riedel: study design pertaining to the design and implementation of the behavioral battery. Manuscript revision and writing. Data revision including statistical analysis.

ACKNOWLEDGMENTS

We acknowledge the charity body "Tenovus Scotland" for financially supporting the project. A big thanks goes to the Aberdeen medical research facility for the great animal care and support provided during the conduct of MPPTP administration and animal behavioral testing. We also tanks the Wellcome Trust UK for having supported Katie J. Clephan with a summer vacation scholarship.

All experiments were conducted in compliance with the ARRIVE guidelines.

CONFLICT OF INTEREST

The authors have no conflict of interest arising from the nature of their work and involvement in other organizations or institutions. No

additional conflict of interest can be derived from the financial support received from the funding body "Tenovus Scotland."

DATA AVAILABILITY STATEMENT

The data that support the findings of this study are available from the corresponding author upon request.

ORCID

Matteo Santoro https://orcid.org/0000-0002-1670-5609

REFERENCES

Aarsland, D., Andersen, K., Larsen, J. P., Lolk, A., & Kragh Sorensen, P. (2003). Prevalence and characteristics of dementia in Parkinson disease: an 8-year prospective study. *Archives of Neurology*, *60*, 387–392.

Aarsland, D., Bronnick, K., Williams Gray, C., Weintraub, D., Marder, K., Kulisevsky, J., Burn, D., Barone, P., Pagonabarraga, J., Allcock, L., Santangelo, G., Foltynie, T., Janvin, C., Larsen, J. P., Barker, R. A., & Emre, M. (2010). Mild cognitive impairment in Parkinson disease: a multicenter pooled analysis. *Neurology*, *75*, 1062–1069.

Anandhan, A., Tamilselvam, K., Vijayraja, D., Ashokkumar, N., Rajasankar, S., & Manivasagam, T. (2010). Resveratrol attenuates oxidative stress and improves behaviour in 1-methyl-4-phenyl-1, 2, 3, 6-tetrahydropyridine (MPTP) challenged mice. *Annals of Neurosciences*, *17*, 113.

Anderson, G., Noorian, A. R., Taylor, G., Anitha, M., Bernhard, D., Srinivasan, S., & Greene, J. G. (2007). Loss of enteric dopaminergic neurons and associated changes in colon motility in an MPTP mouse model of Parkinson's disease. *Experimental Neurology*, *207*, 4–12.

Antzoulatos, E., Jakowec, M. W., Petzinger, G. M., & Wood, R. I. (2010). Sex differences in motor behavior in the MPTP mouse model of Parkinson's disease. *Pharmacology Biochemistry and Behavior*, *95*, 466–472.

Bagga, V., Dunnett, S. B., & Fricker, R. A. (2015). The 6-OHDA mouse model of Parkinson's disease–terminal striatal lesions provide a superior measure of neuronal loss and replacement than median forebrain bundle lesions. *Behavioural Brain Research*, *288*, 107–117.

Bains, R. S., Wells, S., Sillito, R. R., Armstrong, J. D., Cater, H. L., Banks, G., & Nolan, P. M. (2017). Assessing mouse behaviour throughout the light/dark cycle using automated in-cage analysis tools. *Journal of Neuroscience Methods*, *300*, 37–47.

Barone, P., Antonini, A., Colosimo, C., Marconi, R., Morgante, L., Avarello, T. P., Bottacchi, E., Cannas, A., Ceravolo, G., Ceravolo, R., Cicarelli, G., Gaglio, R. M., Giglia, R. M., Iemolo, F., Manfredi, M., Meco, G., Nicoletti, A., Pederzoli, M., Petrone, A., … Group, P. S. (2009). The PRIAMO study: A multicenter assessment of nonmotor symptoms and their impact on quality of life in Parkinson's disease. *Movement Disorders: Official Journal of the Movement Disorder Society*, *24*, 1641–1649.

Bezard, E., Dovero, S., Bioulac, B., & Gross, C. (1997a). Effects of different schedules of MPTP administration on dopaminergic neurodegeneration in mice. *Experimental Neurology*, *148*, 288–292.

Bezard, E., Dovero, S., Bioulac, B., & Gross, C. E. (1997b). Kinetics of nigral degeneration in a chronic model of MPTP-treated mice. *Neuroscience Letters*, *234*, 47–50.

Bohnen, N. I., Albin, R. L., Müller, M. L., Petrou, M., Kotagal, V., Koeppe, R. A., Scott, P. J., & Frey, K. A. (2015). Frequency of cholinergic and caudate nucleus dopaminergic deficits across the predemented cognitive spectrum of Parkinson disease and evidence of interaction effects. *JAMA Neurology*, *72*, 194–200.

Burns, R. S., Chiueh, C. C., Markey, S. P., Ebert, M. H., Jacobowitz, D. M., & Kopin, I. J. (1983). A primate model of parkinsonism: selective destruction of dopaminergic neurons in the pars compacta of the substantia nigra by N-methyl-4-phenyl-1, 2, 3, 6-tetrahydropyridine. *Proceedings of the National Academy of Sciences*, *80*, 4546–4550.

Carta, A. R., Carboni, E., & Spiga, S. (2013). *The MPTP/probenecid model of progressive Parkinson's disease*. Springer.

Chen, J., Song, J., Yuan, P., Tian, Q., Ji, Y., Ren-Patterson, R., Liu, G., Sei, Y., & Weinberger, D. R. (2011). Orientation and cellular distribution of membrane-bound catechol-O-methyltransferase in cortical neurons: implications for drug development. *The Journal of Biological Chemistry*, *286*, 34752–34760.

Chen, M. K., Kuwabara, H., Zhou, Y., Adams, R. J., Brašić, J. R., Mcglothan, J. L., Verina, T., Burton, N. C., Alexander, M., & Kumar, A. (2008). VMAT2 and dopamine neuron loss in a primate model of Parkinson's disease. *Journal of Neurochemistry*, *105*, 78–90.

Claassen, D. O., Josephs, K. A., Ahlskog, J. E., Silber, M. H., TIPPMANN-Peikert, M., & Boeve, B. F. (2010). REM sleep behavior disorder preceding other aspects of synucleinopathies by up to half a century. *Neurology*, *75*, 494–499.

Cohen, G., Pasik, P., Cohen, B., Leist, A., Mytilineou, C., & Yahr, M. D. (1984). Pargyline and deprenyl prevent the neurotoxicity of 1-methyl-4-phenyl-1, 2, 3, 6-tetrahydropyridine (MPTP) in monkeys. *European Journal of Pharmacology*, *106*, 209–210.

Crawley, J., & Goodwin, F. K. (1980). Preliminary report of a simple animal behavior model for the anxiolytic effects of benzodiazepines. *Pharmacology Biochemistry and Behavior*, *13*, 167–170.

Curtin, K., Fleckenstein, A. E., Keeshin, B. R., Yurgelun-Todd, D. A., Renshaw, P. F., Smith, K. R., & Hanson, G. R. (2018). Increased risk of diseases of the basal ganglia and cerebellum in patients with a history of attention-deficit/hyperactivity disorder. *Neuropsychopharmacology*, *43*, 2548–2555.

de Visser, L., van Den Bos, R., Stoker, A. K., Kas, M. J. H., & Spruijt, B. M. (2007). Effects of genetic background and environmental novelty on wheel running as a rewarding behaviour in mice. *Behavioural Brain Research*, *177*, 290–297.

Escola, L., Michelet, T., Douillard, G., Guehl, D., Bioulac, B., & Burbaud, P. (2002). Disruption of the proprioceptive mapping in the medial wall of parkinsonian monkeys. *Annals of Neurology: Official Journal of the American Neurological Association and the Child Neurology Society*, *52*, 581–587.

Espejo, E. F., & Miñano, J. (2001). Adrenergic hyperactivity and metanephrine excess in the nucleus accumbens after prefrontocortical dopamine depletion. *Journal of Neurophysiology*, *85*, 1270–1274.

Fallon, S. J., Gowell, M., Maio, M. R., & Husain, M. (2019). Dopamine affects short-term memory corruption over time in Parkinson's disease. *npj Parkinson's Disease*, *5*, 1–7.

Fifel, K., Dkhissi-Benyahya, O., & Cooper, H. M. (2013). Lack of long-term changes in circadian, locomotor, and cognitive functions in acute and chronic MPTP (1-methyl-4-phenyl-1, 2, 3, 6-tetrahydropyridine) mouse models of Parkinson's disease. *Chronobiology International*, *30*, 741–755.

Filipov, N. M., Norwood, A. B., & Sistrunk, S. C. (2009). Strain-specific sensitivity to MPTP of C57BL/6 and BALB/c mice is age dependent. *Neuroreport*, *20*, 713–717.

Forno, L. S., Langston, J. W., Delanney, L. E., Irwin, I., & Ricaurte, G. A. (1986). Locus ceruleus lesions and eosinophilic inclusions in MPTP-treated monkeys. *Annals of Neurology: Official Journal of the American Neurological Association and the Child Neurology Society*, *20*, 449–455.

George, S., VAN DEN Buuse, M., SAN Mok, S., Masters, C. L., Li, Q.-X., & Culvenor, J. G. (2008). α-Synuclein transgenic mice exhibit reduced anxiety-like behaviour. *Experimental Neurology*, *210*, 788–792.

Gibrat, C., SAINT-Pierre, M., Bousquet, M., Levesque, D., Rouillard, C., & Cicchetti, F. (2009). Differences between subacute and chronic MPTP mice models: investigation of dopaminergic neuronal degeneration and alpha-synuclein inclusions. *Journal of Neurochemistry*, *109*, 1469–1482.

Goldberg, N. R. S., Haack, A. K., Lim, N. S., Janson, O. K., & Meshul, C. K. (2011). Dopaminergic and behavioral correlates of progressive lesioning of the nigrostriatal pathway with 1-methyl-4-phenyl-1, 2, 3, 6-tetrahydropyridine. *Neuroscience*, *180*, 256–271.

Grimbergen, Y. A., Langston, J. W., Roos, R. A., & Bloem, B. R. (2009). Postural instability in Parkinson's disease: the adrenergic hypothesis and the locus coeruleus. *Expert Review of Neurotherapeutics*, *9*, 279–290.

Grubbs, F. E. (1969). Procedures for detecting outlying observations in samples. *Technometrics*, *11*, 1–21.

Guillen, J. (2012). FELASA guidelines and recommendations. *Journal of the American Association for Laboratory Animal Science*, *51*, 311–321.

Haga, H., Matsuo, K., Yabuki, Y., Zhang, C., Han, F., & Fukunaga, K. (2019). Enhancement of ATP production ameliorates motor and cognitive impairments in a mouse model of MPTPâˆ' induced Parkinson's disease. *Neurochemistry International*, *129*, 104492.

Han, N.-R., Kim, Y.-K., Ahn, S., Hwang, T.-Y., Lee, H., & Park, H.-J. (2021). A comprehensive phenotype of non-motor impairments and distribution of alpha-synuclein deposition in parkinsonism-induced mice by a combination injection of MPTP and probenecid. *Frontiers in Aging Neuroscience*, *12*, 512.

Heikkila, R. E., Cabbat, F. S., Manzino, L., & Duvoisin, R. C. (1984). Effects of 1-methyl-4-phenyl-1,2,5,6-tetrahydropyridine on neostriatal dopamine in mice. *Neuropharmacology*, *23*, 711–713.

Huang, D., Xu, J., Wang, J., Tong, J., Bai, X., Li, H., Wang, Z., Huang, Y., Wu, Y., & Yu, M. (2017). Dynamic changes in the nigrostriatal pathway in the MPTP mouse model of Parkinson's disease. *Parkinson's Disease*, *2017*, 7.

Hull, C., Dekeryte, R., Koss, D. J., Crouch, B., Buchanan, H., Delibegovic, M., & Platt, B. (2020). Knock-in of mutated hTAU causes insulin resistance, inflammation and proteostasis disturbance in a mouse model of frontotemporal dementia. *Molecular Neurobiology*, *57*, 539–550.

Irwin, I., Wu, E. Y., Delanney, L. E., Trevor, A., & Langston, J. W. (1987). The effect of diethyldithiocarbamate on the biodisposition of MPTP: an explanation for enhanced neurotoxicity. *European Journal of Pharmacology*, *141*, 209–217.

Jackson-Lewis, V., & Przedborski, S. (2007). Protocol for the MPTP mouse model of Parkinson's disease. *Nature Protocols*, *2*, 141–151.

Janakiraman, U., Manivasagam, T., Thenmozhi, A. J., Essa, M. M., Barathidasan, R., Saravanababu, C., Guillemin, G. J., & Khan, M. A. S. (2016). Influences of chronic mild stress exposure on motor, non-motor impairments and neurochemical variables in specific brain areas of MPTP/probenecid induced neurotoxicity in mice. *PLoS One*, *11*, e0146671.

Jankovic, J. (2003). Pathophysiology and clinical assessment of parkinsonian symptoms and signs. *Neurological Disease and Therapy*, *59*, 71–108.

Kasahara, J., Choudhury, M. E., Nishikawa, N., Tanabe, A., Tsuji, R., Zhou, Y., Ogawa, M., Yokoyama, H., Tanaka, J., & Nomoto, M. (2017). Neurotoxin 1-methyl-4-phenyl-1, 2, 3, 6-tetrahydropyridine (MPTP)-induced animal models of parkinsonâ€™s disease. In *Animal models for the study of human disease*. Elsevier.

Kim, S.-H., Ko, Y. J., & Baek, S.-S. (2021). Resistance exercise improves short-term memory through inactivation of NF-κB pathway in mice with Parkinson disease. *Journal of Exercise Rehabilitation*, *17*, 81–87.

Klingelhoefer, L., & Reichmann, H. (2017). Parkinson's disease as a multisystem disorder. *Journal of Neural Transmission*, *124*, 709–713.

Kurtenbach, S., Wewering, S., Hatt, H., Neuhaus, E. M., & Lübbert, H. (2013). Olfaction in three genetic and two MPTP-induced Parkinson's disease mouse models. *PLoS One*, *8*, e77509.

Lau, Y.-S., Trobough, K. L., Crampton, J. M., & Wilson, J. A. (1990). Effects of probenecid on striatal dopamine depletion in acute and long-term 1-methyl-4-phenyl-1, 2, 3, 6-tetrahydropyridine (MPTP)-treated mice. *General Pharmacology*, *21*, 181–187.

Levine, M., & Ensom, M. H. (2001). Post hoc power analysis: An idea whose time has passed? *Pharmacotherapy: The Journal of Human Pharmacology and Drug Therapy*, *21*, 405–409.

Li, Y., Jiao, Q., Du, X., Bi, M., Han, S., Jiao, L., & Jiang, H. (2018). Investigation of behavioral dysfunctions induced by monoamine depletions in a mouse model of Parkinson's disease. *Frontiers in Cellular Neuroscience*, *12*, 241.

Liu, W. W., Wei, S. Z., Huang, G. D., Liu, L. B., Gu, C., Shen, Y., Wang, X. H., Xia, S. T., Xie, A. M., & Hu, L. F. (2020). BMAL1 regulation of microglia-mediated neuroinflammation in MPTP-induced Parkinson's disease mouse model. *The FASEB Journal*, *34*, 6570–6581.

Liu, X., Liu, S., Tang, Y., Pu, Z., Xiao, H., Gao, J., Yin, Q., Jia, Y., & Bai, Q. (2021). Intragastric administration of casein leads to nigrostriatal disease progressed accompanied with persistent nigrostriatal—intestinal inflammation activited and intestinal microbiota—metabolic disorders induced in MPTP mouse model of Parkinson's disease. *Neurochemical Research*, *46*, 1514–1539.

Lou, Y., Huang, P., Li, D., Cen, Z., Wang, B., Gao, J., Xuan, M., Yu, H., Zhang, M., & Luo, W. (2015). Altered brain network centrality in depressed Parkinson's disease patients. *Movement disorders: Official journal of the Movement Disorder Society*, *30*, 1777–1784.

Luchtman, D. W., Shao, D. I., & Song, C. (2009). Behavior, neurotransmitters and inflammation in three regimens of the MPTP mouse model of Parkinson's disease. *Physiology & Behavior*, *98*, 130–138.

Matheus, F. C., Aguiar, A. S., Jr., Castro, A. A., Villarinho, J. G., Ferreira, J., Figueiredo, C. P., Walz, R., Santos, A. R. S., Tasca, C. I., & Prediger, R. D. S. (2012). Neuroprotective effects of agmatine in mice infused with a single intranasal administration of 1-methyl-4-phenyl-1, 2, 3, 6-tetrahydropyridine (MPTP). *Behavioural Brain Research*, *235*, 263–272.

Mitsumoto, Y., Takamori, S., & Kishida, K. (2019). Psychosocial stress enhances susceptibility to 1-methyl-4-phenyl-1, 2, 3, 6-tetrahydropyridine neurotoxicity in C57BL/6N mice. *Biomedical Research*, *40*, 251–255.

Niewiadomski, W., Palasz, E., Skupinska, M., Zylinski, M., Steczkowska, M., Gasiorowska, A., Niewiadomska, G., & Riedel, G. (2016b). TracMouse: A computer aided movement analysis script for the mouse inverted horizontal grid test. *Scientific Reports*, *6*, 39331.

Nuber, S., Petrasch-Parwez, E., Arias-Carrión, O., Koch, L., Kohl, Z., Schneider, J., Calaminus, C., Dermietzel, R., Samarina, A., & Boy, J. (2011). Olfactory neuron-specific expression of A30P alpha-synuclein exacerbates dopamine deficiency and hyperactivity in a novel conditional model of early Parkinson's disease stages. *Neurobiology of Disease*, *44*, 192–204.

Okano, M., Takahata, K., Sugimoto, J., & Muraoka, S. (2019). Selegiline recovers synaptic plasticity in the medial prefrontal cortex and improves corresponding depression-like behavior in a mouse model of Parkinson's disease. *Frontiers in Behavioral Neuroscience*, *13*, 176.

O'leary, T. P., & Brown, R. E. (2012). The effects of apparatus design and test procedure on learning and memory performance of C57BL/6J mice on the Barnes maze. *Journal of Neuroscience Methods*, *203*, 315–324.

Olivola, E., Pierantozzi, M., Imbriani, P., Liguori, C., Stampanoni Bassi, M., Conti, M., D′ Angelo, V., Mercuri, N. B., & Stefani, A. (2014). Serotonin impairment in CSF of PD patients, without an apparent clinical counterpart. *PLoS One*, *9*, e101763.

Paxinos, G., & Franklin, K. B. J. (2019). *Paxinos and Franklin's the mouse brain in stereotaxic coordinates*. Academic press.

Pessiglione, M., Guehl, D., Rolland, A.-S., François, C., Hirsch, E. C., Féger, J., & Tremblay, L. (2005). Thalamic neuronal activity in dopamine-depleted primates: evidence for a loss of functional segregation within basal ganglia circuits. *Journal of Neuroscience*, *25*, 1523–1531.

Petroske, E., Meredith, G., Callen, S., Totterdell, S., & Lau, Y.-S. (2001). Mouse model of Parkinsonism: a comparison between subacute MPTP and chronic MPTP/probenecid treatment. *Neuroscience*, *106*, 589–601.

Pontone, G. M., Williams, J. R., Anderson, K. E., Chase, G., Goldstein, S. R., Grill, S., Hirsch, E. S., Lehmann, S., Little, J. T., Margolis, R. L., Rabins, P. V., Weiss, H. D., & Marsh, L. (2011). Anxiety and self-perceived health status in Parkinson's disease. *Parkinsonism & Related Disorders*, *17*, 249–254.

Pothakos, K., Kurz, M. J., & Lau, Y.-S. (2009). Restorative effect of endurance exercise on behavioral deficits in the chronic mouse model of Parkinson's disease with severe neurodegeneration. *BMC Neuroscience*, *10*, 1–14.

Prediger, R. D. S., DE-Mello, N., & Takahashi, R. N. (2006). Pilocarpine improves olfactory discrimination and social recognition memory deficits in 24 month-old rats. *European Journal of Pharmacology*, *531*, 176–182.

Prema, A., Janakiraman, U., Manivasagam, T., & Thenmozhi, A. J. (2015). Neuroprotective effect of lycopene against MPTP induced experimental Parkinson's disease in mice. *Neuroscience Letters*, *599*, 12–19.

Przedborski, S., & Vila, M. (2003). The 1-methyl-4-phenyl-1, 2, 3, 6-tetrahydropyridine mouse model: a tool to explore the pathogenesis of Parkinson's disease. *Annals of the New York Academy of Sciences*, *991*, 189–198.

Quinn, L. P., Perren, M. J., Brackenborough, K. T., Woodhams, P. L., Vidgeon-Hart, M., Chapman, H., Pangalos, M. N., Upton, N., & Virley, D. J. (2007). A beam-walking apparatus to assess behavioural impairments in MPTP-treated mice: pharmacological validation with R-(−)-deprenyl. *Journal of Neuroscience Methods*, *164*, 43–49.

Ribeiro, L., Souza, T. M., Bizarro, L., & Oliveira, A. (2011). Proprioceptive deficits in Parkinson's disease: from clinical data to animal experimentation. *Psychology & Neuroscience*, *4*, 235–244.

Richard, I. H. (2005). Anxiety disorders in Parkinson's disease. *Advances in Neurology*, *96*, 42–55.

Robinson, L., Plano, A., Cobb, S., & Riedel, G. (2013). Long-term home cage activity scans reveal lowered exploratory behaviour in symptomatic female Rett mice. *Behavioural Brain Research*, *250*, 148–156.

Rodriguez-Oroz, M. C., Jahanshahi, M., Krack, P., Litvan, I., Macias, R., Bezard, E., & Obeso, J. A. (2009). Initial clinical manifestations of Parkinson's disease: Features and pathophysiological mechanisms. *The Lancet Neurology*, *8*, 1128–1139.

Rosner, B. 2011. *Fundamentals of Biostatistics* (The 7th edition). Brooks/Cole.

Rozas, G., López-Martın, E., Guerra, M. J., & Labandeira-Garcıa, J. L. (1998). The overall rod performance test in the MPTP-treated-mouse model of Parkinsonism. *Journal of Neuroscience Methods*, *83*, 165–175.

Sampaio, T. B., Sari, M. H. M., Pesarico, A. P., Mantovani, A. C., Zeni, G., & Nogueira, C. W. (2018). 7-Fluoro-1, 3-diphenylisoquinoline reverses motor and non-motor symptoms induced by MPTP in mice: role of striatal neuroinflammation. *European Journal of Pharmacology*, *819*, 129–135.

Santoro, M., Maetzler, W., Stathakos, P., Martin, H. L., Hobert, M. A., Rattay, T. W., Gasser, T., Forrester, J. V., Berg, D., & Tracey, K. J. (2016). In-vivo evidence that high mobility group box 1 exerts deleterious effects in the 1-methyl-4-phenyl-1, 2, 3, 6-tetrahydropyridine model and Parkinson's disease which can be attenuated by glycyrrhizin. *Neurobiology of Disease*, *91*, 59–68.

Schamne, M. G., Mack, J. M., Moretti, M., Matheus, F. C., Walz, R., Lanfumey, L., & Prediger, R. D. (2018). The gender-biased effects of intranasal MPTP administration on anhedonic-and depressive-like behaviors in C57BL/6 mice: The role of neurotrophic factors. *Neurotoxicity Research*, *34*, 808–819.

Sedelis, M., Hofele, K., Auburger, G. W., Morgan, S., Huston, J. P., & Schwarting, R. K. (2000). MPTP susceptibility in the mouse: behavioral, neurochemical, and histological analysis of gender and strain differences. *Behavior Genetics*, *30*, 171–182.

Sedelis, M., Schwarting, R. K., & Huston, J. P. (2001). Behavioral phenotyping of the MPTP mouse model of Parkinson's disease. *Behavioural Brain Research*, *125*, 109–125.

Shimada, M. (1981). Alteration of acetylcholine synthesis in mouse brain cortex in mild hypoxie hypoxia. *Journal of Neural Transmission*, *50*, 233–245.

Shin, K. S., Zhao, T. T., Choi, H. S., Hwang, B. Y., Lee, C. K., & Lee, M. K. (2014). Effects of gypenosides on anxiety disorders in MPTP-lesioned mouse model of Parkinson' s disease. *Brain Research*, *1567*, 57–65.

Shulman, L. M., Taback, R. L., Bean, J., & Weiner, W. J. (2001). Comorbidity of the nonmotor symptoms of Parkinson's disease. *Movement Disorders: Official Journal of the Movement Disorder Society*, *16*, 507–510.

Shum, A., Sole, M. J., & VAN Loon, G. R. (1982). Simultaneous measurement of 5-hydroxytryptophan and l-dihydroxyphenylalanine by high-performance liquid chromatography with electrochemical detection: Measurement of serotonin and catecholamine turnover in discrete brain regions. *Journal of Chromatography B: Biomedical Sciences and Applications*, *228*, 123–130.

Spielewoy, C., Roubert, C., Hamon, M., Nosten, M., Betancur, C., & Giros, B. (2000). Behavioural disturbances associated with hyperdopaminergia in dopamine-transporter knockout mice. *Behavioural Pharmacology*, *11*, 279–290.

Stefansky, W. (1972). Rejecting outliers in factorial designs. *Technometrics*, *14*, 469–479.

Strekalova, T., Gorenkova, N., Schunk, E., Dolgov, O., & Bartsch, D. (2006). Selective effects of citalopram in a mouse model of stress-induced anhedonia with a control for chronic stress. *Behavioural Pharmacology*, *17*, 271–287.

Svensson, E., Beiske, A. G., Loge, J. H., Beiske, K. K., & Sivertsen, B. (2012). Sleep problems in Parkinson's disease: A community-based study in Norway. *BMC Neurology*, *12*, 71-2377-12-71.

Tanaka, M., Yamaguchi, E., Takahashi, M., Hashimura, K., Shibata, T., Nakamura, W., & Nakamura, T. J. (2012). Effects of age-related dopaminergic neuron loss in the substantia nigra on the circadian rhythms of locomotor activity in mice. *Neuroscience Research*, *74*, 210–215.

Thanarajah, S. E., Backes, H., Difeliceantonio, A. G., Albus, K., Cremer, A. L., Hanssen, R., Lippert, R. N., Cornely, O. A., Small, D. M., & Brüning, J. C. (2019). Food intake recruits orosensory and post-ingestive dopaminergic circuits to affect eating desire in humans. *Cell Metabolism*, *29*, 695, e4–706.

Tillerson, J. L., Caudle, W. M., Reverón, M. E., & Miller, G. W. (2002). Detection of behavioral impairments correlated to neurochemical deficits in mice treated with moderate doses of 1-methyl-4-phenyl-1, 2, 3, 6-tetrahydropyridine. *Experimental Neurology*, *178*, 80–90.

Tong, J., Meyer, J. H., Furukawa, Y., Boileau, I., Chang, L.-J., Wilson, A. A., & Houle, S. (2013). Distribution of monoamine oxidase proteins in human brain: implications for brain imaging studies. *Journal of Cerebral Blood Flow & Metabolism*, *33*, 863–871.

Tye, K. M., Mirzabekov, J. J., Warden, M. R., Ferenczi, E. A., Tsai, H.-C., Finkelstein, J., Kim, S.-Y., Adhikari, A., Thompson, K. R., & Andalman, A. S. (2013). Dopamine neurons modulate neural encoding and expression of depression-related behaviour. *Nature*, *493*, 537–541.

Volkow, N. D., Wang, G.-J., & Baler, R. D. (2011). Reward, dopamine and the control of food intake: implications for obesity. *Trends in Cognitive Sciences*, *15*, 37–46.

Vučković, M. G., Wood, R. I., Holschneider, D. P., Abernathy, A., Togasaki, D. M., Smith, A., Petzinger, G. M., & Jakowec, M. W. (2008). Memory, mood, dopamine, and serotonin in the 1-methyl-4-phenyl-1, 2, 3, 6-tetrahydropyridine-lesioned mouse model of basal ganglia injury. *Neurobiology of Disease*, *32*, 319–327.

Wang, H., Liang, X., Wang, X., Luo, D., Jia, J., & Wang, X. (2013). Electroacupuncture stimulation improves spontaneous locomotor hyperactivity in MPTP intoxicated mice. *PLoS One*, *8*, e64403.

Wang, X., Xu, J., Wang, Q., Ding, D., Wu, L., Li, Y., Wu, C., & Meng, H. (2021). Chronic stress induced depressive-like behaviors in a

classical murine model of Parkinson's disease. *Behavioural Brain Research*, *399*, 112816.

Wang, X. H., Lu, G., Hu, X., Tsang, K. S., Kwong, W. H., Wu, F. X., Meng, H. W., Jiang, S., Liu, S. W., & Ng, H. K. (2012). Quantitative assessment of gait and neurochemical correlation in a classical murine model of Parkinson's disease. *BMC Neuroscience*, *13*, 142.

Wu, X., Indzhykulian, A. A., Niksch, P. D., Webber, R. M., GARCIA-Gonzalez, M., Watnick, T., Zhou, J., Vollrath, M. A., & Corey, D. P. (2016). Hair-cell mechanotransduction persists in TRP channel knockout mice. *PLoS One*, *11*, e0155577.

Yang, X., Liu, B., Shen, H., Li, S., Zhao, Q., An, R., Hu, F., Ren, H., Xu, Y., & Xu, Z. (2018). Prevalence of restless legs syndrome in Parkinson's disease: a systematic review and meta-analysis of observational studies. *Sleep Medicine*, *43*, 40–46.

Zaczek, R., & Coyle, J. T. (1982). Rapid and simple method for measuring biogenic amines and metabolites in brain homogenates by HPLC-electrochemical detection. *Journal of Neural Transmission*, *53*, 1–5.

Zhang, Q.-S., Heng, Y., Mou, Z., Huang, J.-Y., Yuan, Y.-H., & Chen, N.-H. (2017). Reassessment of subacute MPTP-treated mice as animal model of Parkinson's disease. *Acta Pharmacologica Sinica*, *38*, 1317–1328.

Zhang, X., Bai, L., Zhang, S., Zhou, X., Li, Y., & Bai, J. (2018). Trx-1 ameliorates learning and memory deficits in MPTP-induced Parkinson's disease model in mice. *Free Radical Biology and Medicine*, *124*, 380–387.

Zhang, X., Song, D., Gu, L., Ren, Y., Verkhratsky, A., & Peng, L. (2015). Decrease of gene expression of astrocytic 5-HT2B receptors parallels development of depressive phenotype in a mouse model of Parkinson's disease. *Frontiers in Cellular Neuroscience*, *9*, 388.

Zhao, T. T., Kim, K. S., Shin, K. S., Park, H. J., Kim, H. J., Lee, K. E., & Lee, M. K. (2017). Gypenosides ameliorate memory deficits in MPTP-lesioned mouse model of Parkinsonâ€™s disease treated with L-DOPA. *BMC Complementary and Alternative Medicine*, *17*, 1–9.

Zhou, Z.-L., Jia, X.-B., Sun, M.-F., Zhu, Y.-L., Qiao, C.-M., Zhang, B.-P., Zhao, L.-P., Yang, Q., Cui, C., & Chen, X. (2019). Neuroprotection of fasting mimicking diet on MPTP-induced Parkinson's disease mice via gut microbiota and metabolites. *Neurotherapeutics*, *16*, 741–760.

Zhuang, X., Oosting, R. S., Jones, S. R., Gainetdinov, R. R., Miller, G. W., Caron, M. G., & Hen, R. (2001). Hyperactivity and impaired response habituation in hyperdopaminergic mice. *Proceedings of the National Academy of Sciences of the United States of America*, *98*, 1982–1987.

Zokaei, N., Sillence, A., Kienast, A., Drew, D., Plant, O., Slavkova, E., Manohar, S. G., & Husain, M. (2020). Different patterns of short-term memory deficit in Alzheimer's disease, Parkinson's disease and subjective cognitive impairment. *Cortex*, *132*, 41–50.

Zuddas, A., Corsini, G. U., Schinelli, S., Johannessen, J. N., DI Porzio, U., & Kopin, I. J. (1989). MPTP treatment combined with ethanol or acetaldehyde selectively destroys dopaminergic neurons in mouse substantia nigra. *Brain Research*, *501*, 1–10.

SUPPORTING INFORMATION

Additional supporting information can be found online in the Supporting Information section at the end of this article.

How to cite this article: Santoro, M., Fadda, P., Klephan, K. J., Hull, C., Teismann, P., Platt, B., & Riedel, G. (2023). Neurochemical, histological, and behavioral profiling of the acute, sub-acute, and chronic MPTP mouse model of Parkinson's disease. *Journal of Neurochemistry*, *164*, 121–142. https://doi.org/10.1111/jnc.15699